CHEMISTRY
A European Journal

A Journal of
ChemPubSoc Europe

Accepted Article

Title: Rare-Earth-Metal Pentadienyl Half-Sandwich and Sandwich Tetramethylaluminates – Synthesis, Structure, Reactivity, and Performance in Isoprene Polymerization

Authors: Reiner Anwander, Damir Barisic, Dennis Buschmann, David Schneider, and Cäcilia Maichle-Mössmer

To be cited as: *Chem. Eur. J.* 10.1002/chem.201900108

Link to VoR: http://dx.doi.org/10.1002/chem.201900108

Supported by
ACES

WILEY-VCH

Rare-Earth-Metal Pentadienyl Half-Sandwich and Sandwich Tetramethylaluminates – Synthesis, Structure, Reactivity, and Performance in Isoprene Polymerization

Damir Barisic, Dennis A. Buschmann, David Schneider, Cäcilia Maichle-Mössmer, and Reiner Anwander*

Abstract: Targeting the synthesis of rare-earth metal pentadienyl half-sandwich tetramethylaluminate complexes, homoleptic $Ln(AlMe_4)_3$ (Ln = Y, La, Ce, Pr, Nd, Lu) were treated with equimolar amounts of the potassium salts K(2,4-dmp) (2,4-dmp = 2,4-dimethylpentadienyl), K(2,4-dipp) (2,4-dipp = 2,4-di-*iso*-propylpentadienyl), and K(2,4-dtbp) (2,4-dtbp = 2,4-di-*tert*-butylpentadienyl). The reactions involving the larger rare-earth metal centers lanthanum, cerium, praseodymium, and neodymium gave selectively the desired half-sandwich complexes $[(2,4\text{-dmp})La(AlMe_4)_2]$, $[(2,4\text{-dipp})La(AlMe_4)_2]$, and $[(2,4\text{-dtbp})Ln(AlMe_4)_2]$ (Ln = La, Ce, Pr, Nd) in high crystalline yields. Smaller-sized rare-earth metal centers yielded preferentially the sandwich complexes $[(2,4\text{-dmp})_2Ln(AlMe_4)]$ (Ln = Y, Lu) and $[(2,4\text{-dipp})_2Y(AlMe_4)]$. Activation with fluorinated borate/borane cocatalysts gave highly active catalyst systems for the fabrication of polyisoprene, displaying molecular weight distributions as low as $M_w/M_n = 1.09$ and a maximum *cis*-1,4 selectivity of 90.4%. The equimolar reaction of half-sandwich complex $[(2,4\text{-dtbp})La(AlMe_4)_2]$ with $B(C_6F_5)_3$ led to the isolation and full characterization of the single-component catalyst $\{\{(2,4\text{-dtbp})La[(\mu\text{-Me})_2AlMe(C_6F_5)]\}[Me_2Al(C_6F_5)_2]\}_2$. The reaction of the latter complex with 10 equiv. of isoprene could be monitored by ^1H NMR spectroscopy. Also, a donor-induced aluminato/gallato exchange was achieved with $[(2,4\text{-dtbp})La(AlMe_4)_2]$ and $GaMe_3$ leading to $[(2,4\text{-dtbp})La(GaMe_4)_2]$.

Introduction

Following the report on the first transition metal pentadienyl complex by Pettit and co-workers in 1962,[1] such open variants of the ubiquitous cyclopentadienyl (Cp) congeners have drawn considerable interest throughout the 1980s and 1990s in alkaline,[2] alkaline-earth,[3] main group,[3a] and transition metal chemistry.[4] Most commonly, the unsubstituted pentadienyl and 2,4-dimethylpentadienyl ligands were employed, but *tert*-butyl-,[3c,d,5] phenyl-,[6] CF_3-,[7] trialkylsilyl-,[8] and silyloxy-substituted[9] pentadienyl complexes have been probed as well. Moreover, initial reactivity studies revealed that homoleptic/supported Ti(II), V(II), and Cr(II) pentadienyl complexes $M(2,4\text{-dmp})_2$ display catalysts for ethylene polymerization.[10] Rare-earth metal pentadienyl complexes have been described almost exclusively for the ligands 2,4-dimethylpentadienyl and 2,4-di-*tert*-butylpentadienyl. Examples include the homoleptic complexes $Ln(2,4\text{-dmp})_3$ (Ln = Y, La, Nd, Sm, Gd, Dy, Tb, Er, Lu)[11] and $Ln(2,4\text{-dtbp})_2$ (Ln = Sm, Yb)[12] as well as the divalent donor adducts $[(2,4\text{-dmp})_2Yb(dme)]$[11d] and $[Yb\{1,5\text{-}(Me_3Si)_2C_5H_5\}_2\{diglyme\}]$.[13] Heteroleptic complexes are represented by $[(2,4\text{-dmp})_4Ln_2X_2]$ (Ln = Y; X = Br, Ln = La; X = Br, Ln = Nd; X = Cl, Br, I),[11g] half-open metallocenes such as $[(C_8H_8)Ln(2,4\text{-dmp})(thf)]$ (Ln = Nd, Sm, Er)[14] and a halogenido cluster compound $[Nd_6(2,4\text{-dmp})_6Cl_{12}(thf)_2]$.[15] The complexes $Ln(2,4\text{-dmp})_3$ (Ln = Y, La, Nd), $[(2,4\text{-dmp})LnX]_2$ (Ln = Y; X = Br, Ln = La; X = Br, Ln = Nd; X = Cl, Br, I) and $[Nd_6(2,4\text{-dmp})_6X_{12}(thf)_2]$ (X = Cl, Br) have been scrutinized by Taube and co-workers regarding their performance in butadiene polymerization and proved to be highly efficient precatalysts for the stereoselective fabrication of *cis*-1,4-polybutadiene.[16] The latter study also outlined a mechanism for the activation and subsequent polymerization involving these complexes, proposing halogenido-containing rare-earth metal half-sandwich alkylaluminate complexes as active species (Scheme 1).

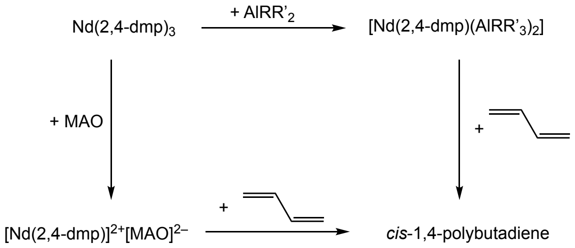

Scheme 1. Activation mechanism of $Nd(2,4\text{-dmp})_3$ with MAO (= methylalumoxane) or $AlRR'_2$ as proposed by Taube et al. (R = halogenido, R' = alkyl).[16]

In the meantime, similar half-sandwich and non-cyclopentadienyl dialkyl complexes have been accessed for a wide range of rare-earth metals, showing excellent performances as precatalysts in butadiene and isoprene polymerization.[17] The rare-earth metal catalyzed coordinative 1,3-diene polymerization draws major interest in scientific and industrial research, as it provides the

---

[*] Damir Barisic, Dennis A. Buschmann, Dr. David Schneider, Dr. Cäcilia Maichle-Mössmer, Prof. Dr. Reiner Anwander
Institut für Anorganische Chemie
Auf der Morgenstelle 18, 72076 Tübingen
E-mail: reiner.anwander@uni-tuebingen.de

Supporting information for this article is given via a link at the end of the document.((Please delete this text if not appropriate)) most efficient initiators with high activity and highly stereoregular polymers.[18] As natural resources cannot satisfy the ever more increasing worldwide demand for polyisoprene, a great deal of research is conducted into highly stereospecific synthesis routes toward synthetic rubber.[17a,18,19] Intrigued and encouraged by the findings of Taube and others, we set out to target rare-earth metal pentadienyl half-sandwich and sandwich tetramethylaluminate chemistry using alternative synthesis approaches. The present study gives a full account of the synthesis of such precatalyst systems as well as their performance in isoprene polymerization including the mechanisms of catalyst activation. We also report on a rare example of a single-component catalyst and a feasible $AlMe_3$/$GaMe_3$ Lewis acid switch. This study is also an extension of our existing bis(tetramethylaluminate) library.[17c-e,20]

Results and Discussion

Synthesis of Ln(III) Pentadienyl Complexes. In contrast to Cp derivatives such as $(C_5Me_5)Ln(AlMe_4)_2$, $(C_5Me_4H)Ln(AlMe_4)_2$, $[1,3\text{-}(Me_3Si)_2C_5H_3]Ln(AlMe_4)_2$, $(C_5Me_4SiMe_3)Ln(AlMe_4)_2$, or $[1,2,4\text{-}(Me_3C)_3C_5H_2]Ln(AlMe_4)_2$, which are readily available via protonolysis of $Ln(AlMe_4)_3$ with the corresponding cyclopentadienes,[17d,21] this protocol was not applicable for Ln(III) pentadienyl half-sandwich complexes. The homoleptic complexes $Ln(AlMe_4)_3$ (Ln = Y, La, Lu) did not react with 2,4-dimethyl-1,3-pentadiene, 2,4-di-*iso*-propyl-1,3-pentadiene, or 2,4-di-*tert*-butyl-1,3-pentadiene, not even at elevated temperatures. Utilizing the salt metathesis route[22] by reacting $La(AlMe_4)_3$ with 0.9 equiv. of the corresponding potassium salts K(2,4-dmp) (2,4-dmp = 2,4-dimethylpentadienyl), K(2,4-dipp) (2,4-dipp = 2,4-di-*iso*-propylpentadienyl), and K(2,4-dtbp) (2,4-dtbp = 2,4-di-*tert*-butylpentadienyl) at low temperature, on the other hand, led to the formation of half-sandwich complexes $[(2,4\text{-dmp})La(AlMe_4)_2]$ (**1**^{La}), $[(2,4\text{-dipp})La(AlMe_4)_2]$ (**2**^{La}), and $[(2,4\text{-dtbp})La(AlMe_4)_2]$ (**3**^{La}), respectively (Scheme 2). Unfortunately, complex **1**^{La} could not be obtained in pure form as a substantial amount of starting material, $La(AlMe_4)_3$, was constantly detected in the proton NMR spectrum. The remainder of the large Ln(III) centers showed a similar reactivity toward K(2,4-dtbp), leading to half-sandwich complexes $[(2,4\text{-dtbp})Ln(AlMe_4)_2]$ (Ln = Ce (**3**^{Ce}), Pr (**3**^{Pr}), Nd (**3**Nd)). Contrary to our expectations, the reaction of one equivalent of K(2,4-dmp) with the smaller lanthanide(III) centers yttrium and lutetium selectively produced the sandwich complexes $[(2,4\text{-dmp})_2Y(AlMe_4)]$ (**4**^{Y}), and $[(2,4\text{-dmp})_2Lu(AlMe_4]$ (**4**^{Lu}), regardless of the reaction temperature. These compounds could also be obtained in higher yields using two equivalents of potassium salt. The same reactivity could be observed for $Y(AlMe_4)_3$ and newly synthesized K(2,4-dipp), leading to sandwich complex $[(2,4\text{-dipp})_2Y(AlMe_4)]$ (**5**), but the $Lu(AlMe_4)_3$–K(2,4-dipp) reaction led only to a mixture of compounds that could not be separated. The reactivity of K(2,4-dtbp) toward the smaller rare-earth metal centers was described recently.[24] A similar size-dependent product distribution in salt metathesis reactions could recently be observed by our group when investigating the formation of rare-earth metal fluorenyl half-sandwich complexes.[20e] A low temperature (–40 °C) and a slight stoichiometric deficiency were crucial for the synthesis of half-sandwich complexes **1**^{La}, **2**^{La}, **3**^{Ln} (Ln = La, Ce, Pr, Nd) as reactions at ambient temperature and/or an equimolar amount of potassium salt led to ligand scrambling and product mixtures. Even dissolution of the half-sandwich complexes in aliphatic or aromatic solvents led to a substantial amount of ligand scrambling over time, with the neodymium compound **3**Nd being the least stable. When dissolving **3**Nd in [D$_6$]benzene for NMR spectroscopic measurements, immediate ligand scrambling to form the sandwich complex $[(2,4\text{-dtbp})_2Nd(AlMe_4)]$ (**6**) and $Nd(AlMe_4)_3$ could be observed (Figure S9). This dynamic behavior is most likely attributable to the neodymium metal size, as ligand redistribution is much less pronounced in solutions of complexes of the larger metal centers lanthanum, cerium, and praseodymium and the fact that the medium-sized yttrium and the small lutetium cations do not form half-sandwich complexes at all. For an unambiguous interpretation of the NMR spectra, the neodymium sandwich complex **6** was synthesized independently from $Nd(AlMe_4)_3$ and two equivalents of potassium salt K(2,4-dtbp) (Scheme 2).

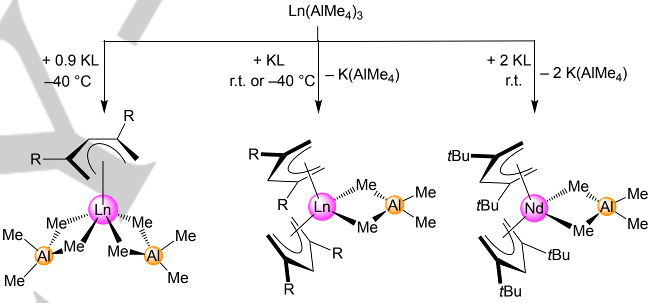

1^{La} (R = Me)
2^{La} (R = *i*Pr)
3^{Ln} (Ln = La, Ce, Pr, Nd; R = *t*Bu)

4^{Ln} (Ln = Y, Lu; R = Me)
5^{Y} (R = *i*Pr)

6

Scheme 2. Synthesis of pentadienyl (L)-supported half-sandwich complexes **1-3** and sandwich complexes **4-6**.

NMR Spectroscopic Investigation of Ln(III) Pentadienyl Complexes. The ^1H NMR spectra obtained from the diamagnetic lanthanum (**1**^{La}, **2**^{La}, **3**^{La}), yttrium (**4**^{Y}, **5**), and lutetium (**4**^{Lu}) complexes show signal ratios of 1:2:2:6 (2,4-dmp), 1:2:2:2:6:6 (2,4-dipp), and 1:2:2:18 (2,4-dtbp), in accordance to the already known homoleptic rare-earth metal pentadienyl complexes.[3d,11g] All complexes show distinct signals for H_c, H_{exo}, and H_{endo} protons (Figure 1) with clear signal splitting for the larger lanthanum(III) complexes except **1**^{La}, which is supported by the sterically least demanding pentadienyl ligand. This indicates a relatively rigid pentadienyl ligand coordination in complexes $[(2,4\text{-dipp})La(AlMe_4)_2]$ and $[(2,4\text{-dtbp})La(AlMe_4)_2]$. On the other hand, complex **1**^{La} and the ones with the smaller yttrium(III) and lutetium(III) centers (**4**^{Y}, **4**^{Lu}) show only singlets for the pentadienyl protons, pointing to a more dynamic behavior (**4**^{Lu} gave singlets at even -80 °C). This behavior could originate from an η^5–η^1–η^5 shift of the ligand, or ligand "flipping", as previously described by Ernst in 1985.[4a] Only one signal in the range of –0.36 to –0.04 ppm was observed for the $[AlMe_4]$ moiety in all complexes except for the sandwich complex **4^{Lu}** with the smallest Ln(III) cation, where two signals – for bridging and terminal methyl groups – are present. Furthermore, the 2,4-di-*iso*-propylpentadienyl ligand in complexes **2^{La}** and **5** shows two distinct signals for the methyl groups of the isopropyl substituent, also indicating a restricted mobility. In addition, the yttrium(III) complexes show a $^2J_{H,Y}$ coupling of 1.78 Hz (**4^{Y}**, **5**) for the [AlMe$_4$] groups, respectively, characteristic of yttrium tetramethylaluminate complexes.[19b,20e]

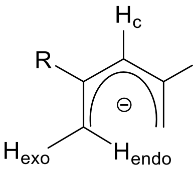

Figure 1. Proton assignment in pentadienyl ligands.

X-Ray Structure Analyses of Ln(III) Pentadienyl Half-Sandwich Complexes. All isolated half-sandwich complexes were examined by X-ray structure crystallography. Single crystals were obtained from saturated *n*-hexane/TMS solutions at –40 °C. The molecular structures of [(2,4-dmp)La(AlMe$_4$)$_2$] (**1^{La}**), [(2,4-dipp)La(AlMe$_4$)$_2$] (**2^{La}**), and [(2,4-dtbp)La(AlMe$_4$)$_2$] (**3^{La}**) are depicted in Figure 2; those of complexes **3^{Ce}** and **3^{Pr}** are isostructural to **3^{La}**, and shown in the supporting information (Figures S38 and S39). Complex **3Nd** crystallized in a different space group, but is isostructural to the other half-sandwich complexes (Figure S40). Selected bond lengths for the lanthanum half-sandwich complexes are given in Table 1. All half-sandwich complexes show the structural motif already observed for cyclopentadienyl- and fluorenyl-supported half-sandwich complexes.[17d,e,20e] The pentadienyl ligand coordinates in a U-shaped η^5-fashion to the metal center. This U-shape is typical for pentadienyl ligands and was also observed previously for homo- and heteroleptic rare-earth metal pentadienyl complexes such as Ln(2,4-dmp)$_3$ (Ln = Y, La, Nd, Gd, Dy, Tb, Er, Lu)[11a-g], [Ln(2,4-dtbp)$_2$(do)] (Ln = Sm, Yb; do = thf, dme)[12], or [(2,4-dmp)$_2$LnX]$_2$ (Ln = Y, Nd, Gd; X = Cl, Br, I).[11g,24] At first glance, all pentadienyl half-sandwich complexes under study seem to feature 7-coordinate rare-earth metal centers. However, an η^3-coordination by one [AlMe$_4$] ligand likely compensates for enhanced steric unsaturation of the lanthanum centers in complexes **1^{La}** (La···C10 = 3.083(4) Å; torsion angles: La–C8–Al1–C9 = 50.62 °; La–C12–Al2–C13 = 8.96 °) and **2^{La}** (La···C14 = 3.106(7) Å; torsion angles: La–C12–Al1–C13 = –51.59 °; La–C16–Al2–C17 = –9.41 °). This interaction is only observed in the solid state.[20b] In complexes **3^{Ln}**, the bulkier 2,4-dtbp ligand apparently prevents such an η^3-coordination, causing both [AlMe$_4$] groups to adopt an η^2-coordination (torsion angles for **3^{La}**: La–C14–Al1–C15 = –6.32 °; La–C18–Al2–C19 = 14.44 °). Compared to the Cp ligand in [(C$_5$Me$_5$)La(AlMe$_4$)$_2$] (La–C(C$_5$Me$_5$)), 2.753(2)–2.801(3) Å),[21a] the pentadienyl ligand in complexes **1^{La}**, **2^{La}**, and **3^{La}** seems positioned further away from the metal center. In particular, the central C3 atom in **3^{La}** is found comparatively close to the lanthanum center– the probable cause being the higher charge density located on the latter. When comparing complexes **1^{La}**, **2^{La}**, and **3^{La}**, it should be noted that the metal-centroid distance decreases with increasing substituent size (**1^{La}** > **2^{La}** > **3^{La}**), attributable to opposing effects, the ability of the sterically more demanding substituents *i*Pr and *t*Bu to interact with the metal center via peripheral methyl groups, and a concomitant η^3/η^2-coordination switch of the aluminato ligand.

X-Ray Structure Analyses of Ln(III) Pentadienyl Sandwich Complexes. In the solid state, complexes **4^{Y}** and **4^{Lu}** are isostructural (Figures 3/top and S41) with a gauche conformation of the two pentadienyl ligands toward each other (conformation angle χ·= 46°).[3d] Complex **5** shows a similar structure in which the pentadienyl ligands adopt an eclipsed conformation (χ·= 1°), however, with the *i*Pr groups pointing away from each other (Figure 3/bottom). The even more bulky 2,4-di-*tert*-butyl-pentadienyl ligand in complex **6** conversely has a conformation angle of 46° (Figure S42). The different conformation in complex **5** involves a possible interaction between the CH protons H17 and H20 of the *i*Pr groups with the negatively charged carbon atoms C1 and C5 (C1···H20 = 2.860(9) Å; C5···H17 = 2.881(2) Å), "locking" the ligands in place as a result (Figure 3). The [AlMe$_4$] groups in these complexes show an η^2-planar coordination mode (**6**), which is characteristic of lanthanidocene tetramethylaluminate complexes[25] and an η^2-bent coordination mode (**4^{Y}**, **4^{Lu}**, and **5**), most likely due to the Me and *i*Pr groups of complexes **4** and **5** being sterically less demanding than the *t*Bu groups of **6**, thus allowing approach of an additional CH$_3$ group to the rare-earth-metal center (e.g., C25 in complex **5**).

Table 1. Selected interatomic distances [Å] of **1^{La}**, **2^{La}**, and **3^{La}**

	1^{La}	**2^{La}**	**3^{La}**
La···Ct	2.416	2.410	2.386
La–C1	2.818(3)	2.856(4)	2.906(2)
La–C2	2.874(3)	2.894(5)	2.872(2)
La–C3	2.783(3)	2.734(9)	2.668(2)
La–C4	2.924(3)	2.890(0)	2.852(2)
La–C5	2.880(4)	2.874(8)	2.844(2)
La···Al1	3.020(4)	3.029(8)	3.289(4)
La···Al2	3.246(2)	3.225(6)	3.274(2)
La–C8/13/14	2.841(4)	2.875(5)	2.713(2)
La–C9/12/15	2.853(4)	2.847(0)	2.764(2)
La–C10/14/16	3.083(4)	3.106(7)	4.625(2)
La–C12/17/19	2.715(4)	2.680(6)	2.716(2)
La–C13/16/18	2.722(4)	2.680(5)	2.726(2)

10.1002/chem.201900108

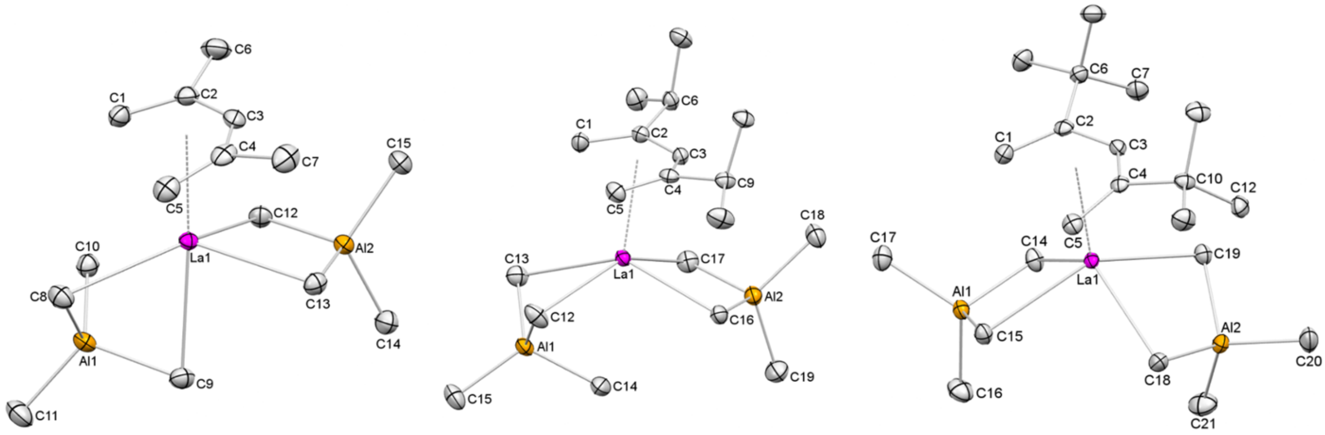

Figure 2. Molecular structures of [(2,4-dmp)La(AlMe$_4$)$_2$] (**1^{La}**, left), [(2,4-dipp)La(AlMe$_4$)$_2$] (**2^{La}**, middle), and [(2,4-dtbp)La(AlMe$_4$)$_2$] (**3^{La}**, right); complexes **3^{Ce}**, **3^{Pr}**, and **3Nd** are isostructural (Figures S38, S39, and S40). Hydrogen atoms are omitted for clarity. Atomic displacement parameters are set at the 50% probability level. Selected bond lengths are given in Table 1.

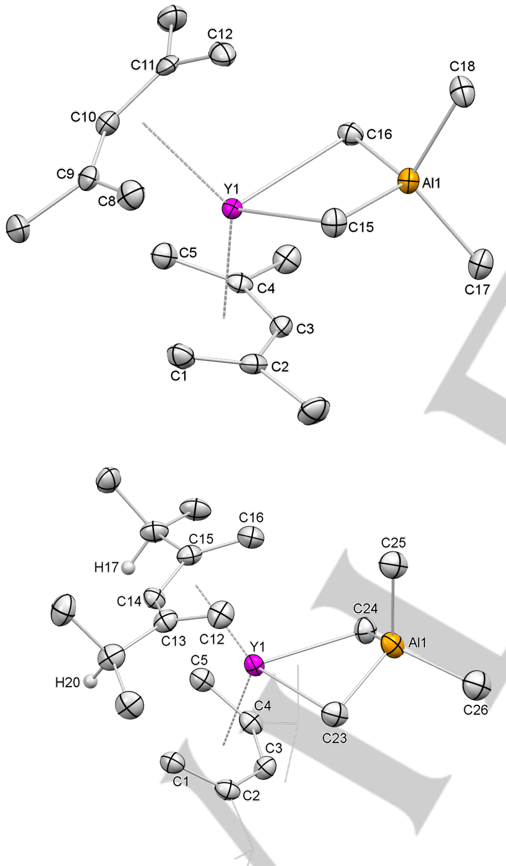

Figure 3. Molecular Structure of **4^{Y}** and **5^{Y}** with atomic displacement parameters set at the 50% level. For **5^{Y}** hydrogen atoms except for H17 and H20 and *i*Pr groups of one pentadienyl ligand are omitted for clarity. Selected interatomic distances [Å] and angles [°]: **4^{Y}**: Y–C1 2.709(3); Y–C2 2.702(2); Y–C3 2.599(2); Y–C4 2.702(2); Y–C5 2.704(2); Y–C8 2.727(3); Y–C9 2.698(2); Y–C10 2.594(2); Y–C11 2.703(3); Y–C12 2.808(3); Y–C15 2.593(3); Y–C16 2.677(3); Y···Al 3.097(1); Al–C15 2.067(3); Al–C16 2.065(2); Al–C17 1.975(3); Al–C18 1.975(2); C1–C2 1.370(3); C2–C3 1.430(3); C3–C4 1.429(3); C4–C5 1.377(3); C8–C9 1.377(4); C9–C10 1.421(4); C10–C11 1.432(3); C11–C12 1.355(4); Ct1–Y–Ct2 133.4(4); Y–C15–Al 82.4(6); Y–C16–Al 80.4(2); C15–Y–C16 81.6(4); C15–Al–C16 112.9(9). **5^{Y}**: Y–C1 2.659(3); Y–C2 2.719(3); Y–C3 2.599(3); Y–C4 2.732(3); Y–C5 2.704(3); Y–C12 2.772(3); Y–C13 2.738(3); Y–C14 2.579(3); Y–C15 2.730(3); Y–C16 2.717(4); Y–C23 2.641(4); Y–C24 2.660(4); Y···C25 4.138(8); Y···H17 3.902(1); Y···H20 3.849(3); Y···Al 3.102(7); Al–C23 2.061(4); Al–C24 2.065(4); Al–C25 1.994(4); Al–C26 1.975(4); C1–C2 1.382(5); C2–C3 1.425(4); C3–C4 1.439(4); C4–C5 1.378(5); C12–C13 1.368(5); C13–C14 1.440(4); C14–C15 1.428(4); C15–C16 1.368(5); Ct1–Y–Ct2 128.4(2); Y–C23–Al 81.5(8); Y–C24–Al 81.0(4); C23–Y–C24 77.7(8); C23–Al–C24 107.5(3).

Reactivity of [(2,4-dtbp)La(AlMe$_4$)$_2$] (3^{La}) toward GaMe$_3$. To examine the feasibility of a donor-assisted tetramethylaluminato/gallato exchange, the half-sandwich pentadienyl complex **3^{La}** was treated with an excess of GaMe$_3$ and three equivalents of diethyl ether. This reaction protocol was utilized earlier by our group to gain access to tetramethylgallate complexes of the early rare-earth metals, demonstrating that diethyl ether binds more strongly to trimethylaluminum than trimethylgallium.[26] Indeed, the reaction proceeded as expected to generate the lanthanum half-sandwich pentadienyl tetramethylgallate complex [(2,4-dtbp)La(GaMe$_4$)$_2$] (**7**) (Scheme 3).

However, despite several recrystallization attempts, complex **7** remained contaminated with a significant amount of an unknown by-product, as evident from distinct methyl signals in the variable temperature ^{1}H NMR spectrum (Figures S19, S20, and S37). X-ray structure analysis of complex **7** revealed a similar structural motif as observed for the corresponding tetramethylaluminate complex **3^{La}** (Figure 4). However, one of the [GaMe$_4$] groups in **7** exhibits an η^2-bent coordination, owing to the lower Lewis acidity of gallium(III) compared to aluminum(III) and, as a result, less repulsion between the two metal centers. This distinct tetramethylgallato coordination also causes the pentadienyl ligand to be located further away from the lanthanum(III) center than in parent complex **3^{La}** while retaining its typical U-shaped η^5-

coordination. A similar tetramethylgallato coordination was already observed for $[(C_5Me_5)La(GaMe_4)_2]$.[26]

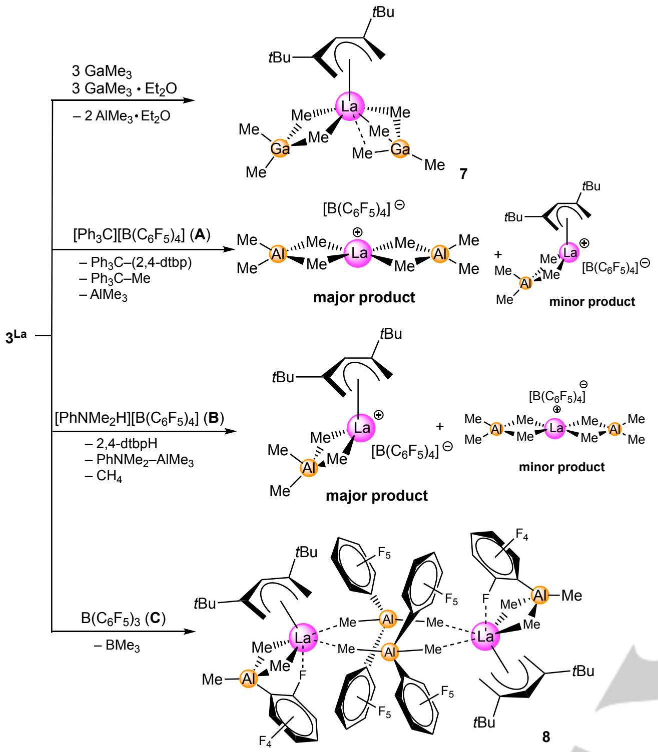

Scheme 3. Synthesis of Bis(gallate) $[(2,4\text{-dtbp})La(GaMe_4)_2]$ (**7**) and equimolar activation reactions of **3^{La}** with perfluorinated borates **A** and **B** as well as borane **C**, including the formation of $\{\{(2,4\text{-dtbp})La[(\mu\text{-}Me)_2AlMe(C_6F_5)]\}[Me_2Al(C_6F_5)_2]\}_2$ (**8**). For reactions **3^{La}**/**A** and **3^{La}**/**B** proposed species only.

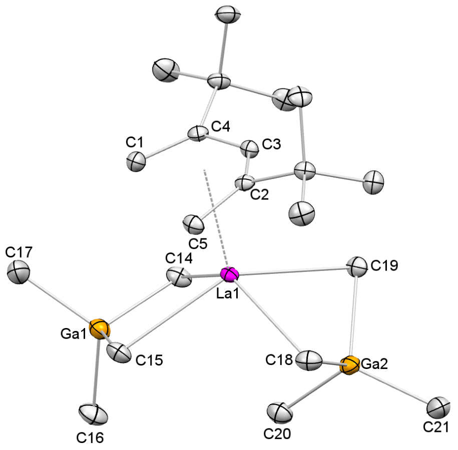

Figure 4. Molecular Structure of **7** with atomic displacement parameters set at the 50% level. Hydrogen atoms are omitted for clarity. Selected interatomic distances [Å] and angles [°]: La–C1 2.936(3); La–C2 2.896(2); La–C3 2.709(3); La–C4 2.879(3); La–C5 2.856(3); La–C14 2.717(3); La–C15 2.736(3); La–C18 2.833(3); La–C19 2.743(3); La···C20 3.257(3) La···Ga1 3.254(1); La···Ga2 3.027(1); Ga1–C14 2.101(3); Ga1–C15 2.096(3); Ga1–C16 1.978(3); Ga1–C17 1.985(3); Ga2–C18 2.074(3); Ga2–C19 2.090(3); Ga2–C20 2.018(3); Ga2–C21 1.967(3); C1–C2 1.364(3); C2–C3 1.449(3); C3–C4 1.428(3); C4–C5 1.379(3); Ct–La–Ga1 110.6(6); Ct–La–Ga2 136.7(5); La–C14–Ga1 83.5(6); La–C15–Ga1 83.9(3); C14–La–C15 79.4(8); C14–Ga1–C15 112.3(9); La–C18–Ga2 76.2(1); La–C19–Ga2 74.3(7); C18–La–C19 73.7(2); C18–Ga2–C19 106.9(3).

Polymerization of Isoprene and Investigation of Active Species. Earlier studies conducted by our group revealed that half-sandwich rare-earth metal tetramethylaluminate complexes $[Cp^RLn(AlMe_4)_2]$ (Ln = Y, La, Nd, Lu) polymerize isoprene efficiently when cationized with borate cocatalysts $[CPh_3][B(C_6F_5)_4]$ (**A**), $[PhNMe_2H][B(C_6F_5)_4]$ (**B**), and $B(C_6F_5)_3$ (**C**).[17c-e,20e] Since homoleptic 2,4-dimethylpentadienyl complexes of the rare-earth metals (Ln = La, Nd, Y) were investigated by Taube et al. regarding the polymerization of butadiene,[16] we were interested in studying the polymerization performance of the half-sandwich pentadienyl complexes **2^{La}**, **3^{La}**, **3^{Ce}**, and **3Nd**. We refrained from probing complex **1^{La}** in this regard, as it could not be isolated in pure form. Also, direct addition of isoprene to a solution of the half-sandwich complexes or activation with chloride-based cocatalyst such as Me_2AlCl or Et_2AlCl did not lead to a polymerization reaction (catalyst preformation times up to 30 minutes). An ^{1}H NMR spectroscopic study of an equimolar reaction mixture of **3^{La}** and Me_2AlCl indicated the formation of a mixture of unreacted half-sandwich complex, metallocene complex $[(2,4\text{-dtbp})_2La(AlMe_4)]$, $[(2,4\text{-dtbp})_2AlMe]$, $AlMe_3$, and $LaCl_3$ (elemental analysis/Figure S25). Therefore, as a general procedure, the complexes were activated by addition of one or two equivalents of borate/borane cocatalysts **A**, **B**, or **C** to the respective toluene solutions prior to testing for the homopolymerization of isoprene. The polymerization results are summarized in Tables 2, S4 and S5.

To investigate if the active species correspond to those revealed for cyclopentadienyl-supported catalysts,[17c,e] NMR-scale reactions were conducted with compound **3^{La}** and an equimolar and double-molar amount of cocatalysts **A**-**C**. Activation of **3^{La}** with cocatalyst **A** led to abstraction of the pentadienyl ligand and formation of Ph_3C–(2,4-dtbp) as the main product along with the same active species that can be found when activating $La(AlMe_4)_3$ with cocatalyst **A** (Scheme 3).[19e] The solid-state structure of Ph_3C–(2,4-dtbp) could be determined by X-ray crystallographic analysis and is shown in Figure S43. Another activation by-product, Ph_3C–Me, derived from the abstraction of one $[AlMe_4]$ methyl group could also be detected as a minor product as could be a third species in the ^{19}F NMR spectrum. Such abstraction of supposedly/putative ancillary ligands was previously described for the activation of half-sandwich fluorenyl and indenyl complexes.[27] Interestingly, the polymer microstructure derived from catalyst system **3^{La}**/**A** was almost identical to the one derived from $La(AlMe_4)_3$/**A**[19e] although at least three different species are present in the reaction mixture (Table 2, entry 7). The addition of another equivalent of borate cocatalyst **A** led to the disappearance of the signals of the active species mentioned above and a large $AlMe_3$ signal appeared in the proton NMR spectrum. Signals of Ph_3C–(2,4-dtbp) and Ph_3C–Me were still

10.1002/chem.201900108

present, with the amount of Ph_3C–Me being significantly larger than in the equimolar catalyst system, caused by an additional abstraction of a methyl group by the cocatalyst. The ^{19}F NMR spectrum of the catalyst system **3**^{La}/2**A** shows only one set of signals and thus only one active species as opposed to the equimolar catalyst system.

Activation of **3**^{La} with cocatalyst **B** gave a significantly different activation pattern with the main products detectable in the ^{1}H NMR spectrum being the ionic species [(2,4-dtbp)La($AlMe_4$)][B(C_6F_5)$_4$] and the trimethylaluminum dimethylanilinium adduct $PhNMe_2$–$AlMe_3$ (Scheme 3). As a minor side product, the proligand 2,4-di-*tert*-butyl-1,3-pentadiene (2,4-dtbpH) could also be observed and three different signal sets are present in the ^{19}F NMR spectrum (*cf.,* equimolar activation with **A**). Addition of another equivalent of cocatalyst **B** resulted in increasing amounts of 2,4-dtbpH in the ^{1}H NMR spectrum, corresponding to further protonation of the active species [(2,4-dtbp)La($AlMe_4$)][B(C_6F_5)$_4$] and leading to the formation of a species similar to that in system **3**^{La}/2**A**. The ^{19}F NMR spectrum of the mixture **3**^{La}/2**B** shows two different signal sets, indicative of the co-existence of two distinct species.

Equimolar treatment of **3**^{La} with borane **C** led to the formation of isolable compound {{(2,4-dtbp)La[(μ-Me)$_2$AlMe(C_6F_5)]}[$Me_2Al(C_6F_5)_2$]}$_2$ (**8**), which was further characterized by NMR spectroscopy and X-ray crystallography (Scheme 3 and Figure 5).

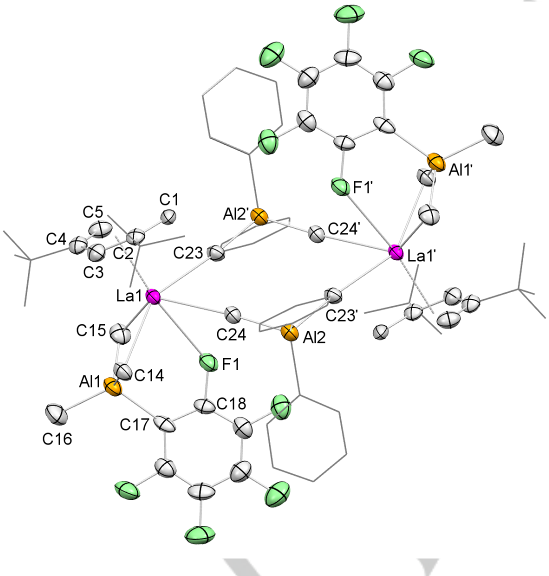

Figure 5. Molecular Structure of **8** with atomic displacement parameters set at the 50% level. Hydrogen atoms and crystal lattice toluene are omitted for clarity. Selected interatomic distances [Å] and angles [°]: La–C1 2.890(6); La–C2 2.858(6); La–C3 2.676(6); La–C4 2.837(6); La–C5 2.805(6); La–C14 2.673(7); La–C15 2.725(8); La–C23 2.886(6); La–C24 2.929(7); La···F1 2.957(4); La···Al1 3.252(2); F1–C18 1.385(7); Al1–C14 2.050(8); Al1–C15 2.031(9); Al1–C16 1.979(7); Al1–C17 2.019(7); La1···La1' 7.692; Ct–La1–Al1 127.6(9); Ct–La1–F1 171.2(9); La1–C14–Al1 85.9(8); La–C15–Al1 84.9(5); C14–Al1–C15 110.6(3); C14–La1–C15 76.8(7); C23–Al2–C24' 105.7(7); La1–C23–Al2 171.9(1); C24–La1–C23 78.6(2)

A structurally similar complex could be isolated earlier by us from the reaction of [(C_5Me_5)La($AlMe_4$)$_2$] and B(C_6F_5)$_3$.[17c] In the solid state, complex **8** features a dimeric structure with two [(C_6F_5)$_2$AlMe$_2$] units bridging between the lanthanum centers forming a contact ion pair. A single Me/[C_6F_5] exchange occurred also within the terminal alkyl aluminate moiety, which exhibits one *ortho*-fluorine atom interaction with the lanthanum center. The 2,4-dtbp ligand retained its U-shaped η^{5}-coordination.

In contrast to the C_5Me_5-supported complex, **8** shows dynamic behavior in solution with a monomer-dimer equilibrium at ambient temperature. The signals of the pentadienyl backbone appear much broader in the dimer than those of the monomer as the large [C_6F_5] groups and the resulting steric pressure probably facilitate a dynamic behavior of the ligand. The dynamic behavior and hence less tightly bonded contact ion pairs are also reflected in the substantially weaker interactions between the lanthanum center and the terminal and bridging heteroaluminato ligands [(C_6F_5)AlMe$_3$] and [(C_6F_5)$_2$AlMe$_2$], respectively. The La–C(methyl) (2.673(7)–2.929(7) Å) and La···F distances (2.957(4) Å) are significantly longer than in the corresponding cyclopentadienyl complex (2.62(1)–2.79(1) Å and 2.62(1) Å).[17c] The La···F interaction is not retained in solution as the ^{19}F NMR spectrum shows only two signal sets for *ortho*, *para*, and *meta*-fluorine atoms. VT NMR spectroscopic measurements indicated a decrease of and subsequent disappearance of the monomer signals corroborating that the dimeric structure is the predominant species at lower temperatures (Figure S36). Complex **8** polymerizes isoprene without addition of any activating agent and thus features a rare single-molecule/component catalyst (cf., vide infra). A ^{1}H NMR-scale experiment with 10 equivalents of isoprene added to a [D_8]toluene solution of **8** over the course of 5 h (Figure 6) revealed a very slow polymerization initiation rate, with polyisoprene signals starting to appear after 45 min and subsequent disappearance of the terminal methyl group signal at 0.56 ppm, implicating that isoprene is inserted into a La–Me bond rather than in between the La(III) center and the pentadienyl ligand.[17c]

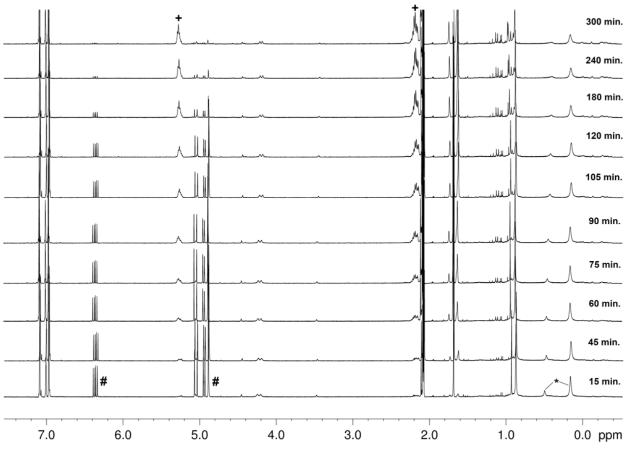

Figure 6. ^{1}H NMR spectra of the reaction of 10 equiv. isoprene with **8** monitored over the course of 5 h. Asterisk for the methyl groups of **8**, **#** for isoprene, **+** for polyisoprene.

10.1002/chem.201900108

On the other hand, multiple signals in the *t*Bu region between 0.97 and 1.21 ppm emerged when polyisoprene started to form. These findings might be explained by either 1) that at some point, the polyisoprene chain does insert in between the metal center and the pentadienyl ligand after all or 2) decomposition of the catalyst.

Catalyst system **3**^{La}/2**C** afforded polyisoprenes with the highest *cis*-1,4 content, pointing to a coordinatively unsaturated lanthanum center catalyst (cf., vide supra). The nature of the active catalyst present in the reaction mixture could not be determined but ^{1}H NMR spectroscopy revealed again the formation of BMe_3 (δ = 0.67 ppm, Figure S34). Furthermore, at least three individual *t*Bu signals are also detected in the spectrum, indicating a mixture of compounds. This is also underlined by the presence of three signal sets in the ^{19}F NMR spectrum.

Effect of the Cocatalyst. In general, all tested complexes **2**^{La}, **3**^{La}, **3**^{Ce}, and **3**Nd afforded high polymer yields (>92%) and relatively narrow molecular weight distributions M_w/M_n (<2.00) with all three cocatalysts **A**, **B**, and **C** (Table 2). Equimolar amounts of cocatalysts **A**, **B**, and **C** gave polymers with a relatively equal *cis*- and *trans*-content distribution (Table 2, entries 1, 3, 5, 7, 9, and 11; Table S4, entries 14, 16, 18, 20, 22, and 24), whereas an additional equivalent of cocatalyst led to higher *cis* and 3,4-selectivities (Table 2, entries 2, 4, 6, 8, 10, and 12, Table S4, entries 15, 17, 19, 21, 23, and 25), corresponding to increasingly unsaturated rare-earth metal centers. Entries 2 (**2**^{La}/2**A**) and 21 (**3**Nd/2**A**) stand out as they show a broader polydispersity index M_w/M_n of 2.24 and 2.19, respectively. A double-molar amount of cocatalyst **C** (entries 6, 12, 19, and 25) gave rise to the highest *cis*- and lowest *trans*-polyisoprene contents with the highest *cis*-polyisoprene content of 90% for the system **2**^{La}/2**C** (entry 6). Complex **8** features a single-component catalyst, producing a polyisoprene with a higher *trans*-content, as opposed to that of the binary system **3**^{La}/**C** (entries 11 versus 13). For comparison, cyclopentadienyl-supported bis(tetramethylaluminate) complexes of the larger rare-earth metal centers when combined with cocatalysts **B** and **C** afford mainly *trans*-polyisoprene.[17c-e] The higher *cis*-polyisoprene contents in the present catalyst systems are yet another hint to the importance of the supporting ligand in isoprene polymerization. As the pentadienyl ligands can be regarded as “open” cyclopentadienyl systems, they allow for more space above the metal center, thus facilitating an *anti*-coordination of the polymer chain and a *cis*-1,4-insertion of isoprene into the growing chain.[29]

Effect of the Pentadienyl Ligand. A change in the substitution pattern on positions C2 and C4 of the pentadienyl ligand from *t*Bu to the sterically less demanding *i*Pr substituent (Table 2, entries 1-6) did not result in a significant change of the polyisoprene microstructure. The only catalyst system that showed a marked difference when changing from *t*Bu to *i*Pr was **2**^{La}/2**A**, which exhibited a considerably larger M_w/M_n value (2.24) compared to the corresponding catalyst system **3**^{La}/2**A** (1.23). Of note should be the slightly minor yields of **2**^{La} (92-98%) in comparison with **3**^{La} (99%). The largely non-existent influence of the substitution pattern on the pentadienyl ligand on the polymerization outcome could be expected as the substituents on C2 and C4 point away from the active site of the catalyst.

Table 2. Polymerization of isoprene by lanthanum pentadienyl complexes **2**^{La}, **3**^{La}, and **8**

entry[a]	precatalyst	cocatalyst[b]	yield [%]	*trans*-1,4–[c]	*cis*-1,4–[c]	3,4–[c]	M_n (x 10^3)[d]	M_w/M_n[d]	T_g [°C][e]	eff.[f]
1	**2**^{La}	**A**	95	50.1	46.1	3.8	51.3	1.16	–64.2	1.33
2	**2**^{La}	2**A**	98	5.0	79.4	15.6	137.4	2.24	–51.4	0.50
3	**2**^{La}	**B**	92	55.3	41.0	3.7	43.5	1.21	–60.1	1.56
4	**2**^{La}	2**B**	97	21.3	67.7	11.0	40.4	1.14	–56.4	1.68
5	**2**^{La}	**C**	95	41.8	55.6	2.6	75.4	1.15	–63.6	0.90
6	**2**^{La}	2**C**	95	3.1	90.4	6.5	68.0	1.09	–58.7	1.00
7	**3**^{La}	**A**	>99	52.0	44.1	3.9	47.0	1.12	–61.9	1.45
8	**3**^{La}	2**A**	>99	8.9	76.8	14.3	61.6	1.23	–49.9	1.10
9	**3**^{La}	**B**	>99	51.7	43.6	4.7	43.8	1.10	–61.8	1.55
10	**3**^{La}	2**B**	>99	23.4	66.7	9.9	55.9	1.10	–55.4	1.22
11	**3**^{La}	**C**	>99	41.7	55.4	2.9	66.9	1.15	–61.4	1.02
12	**3**^{La}	2**C**	99	5.4	88.1	6.6	78.5	1.14	–57.8	0.87
13	**8**	-	>99	51.4	46.0	2.6	38.6	1.10	–64.2	1.76

[a]General polymerization procedure: 0.02 mmol of precatalyst, 8 mL of toluene, 20 mmol of isoprene, 2 h, 40 °C; [b]A = $[CPh_3][B(C_6F_5)_4]$; B = $[PhNMe_2H][B(C_6F_5)_4]$; C = $B(C_6F_5)_3$; catalyst preformation: 30 min. [c]Determined by ^{1}H and ^{13}C NMR spectroscopy in $CDCl_3$. [d]Determined by GPC against polystyrene standards ($M_{n,theory}$ = 68.0 x 10^3 $molL^{-1}$). Assuming a living polymerization: 68[e] Determined by DSC at 20 K/min. [f] Initiation efficiency = M_n(calculated)/M_n(measured).

10.1002/chem.201900108

Effect of the Rare-Earth Metal Center in Complexes $\mathbf{3^{La}}$-$\mathbf{3^{Nd}}$. The decrease in metal center size from lanthanum ($\mathbf{3^{La}}$) over cerium ($\mathbf{3^{Ce}}$) to neodymium ($\mathbf{3^{Nd}}$) in equimolar catalyst systems (cocatalysts **B** and **C**) resulted in an increase of the *cis*-content and a subsequent decrease of the *trans*-content in the polyisoprenes (entries 9, 11, 16, 18, 22, and 24). This is in good agreement with results of earlier isoprene polymerization studies of Cp^R-supported half-sandwich complexes, in which the even smaller rare-earth metal centers yttrium and lutetium showed a significant *cis*-1,4-polyisoprene selectivity.[17c,20e] Interestingly, for the systems with two equivalents of cocatalyst, the *cis*-content decreased for the catalyst systems $\mathbf{3^{Ce}}$/2**B** (entry 17) and $\mathbf{3^{Ce}}$/2**C** (entry 19) in comparison to the lanthanum and neodymium analogues (entries 10, 12, 23, and 25). Also, lower polymer yields were found for the cerium containing catalyst systems compared to lanthanum and neodymium.

Performance of of Ln(III) Pentadienyl Metallocene Complexes. Representative polymerization reactions were also run with the open sandwich complexes $\mathbf{4^{Y}}$ and $\mathbf{4^{Lu}}$ (Table S5). Only a few examples of such "monoalkyl" species were previously shown to be capable of polymerizing 1,3-dienes.[20d] These rare examples are limited to the dimeric complexes $[(C_5Me_4)_2Ln(\mu\text{-}Me)_2AlMe_2]_2$[29] and $[(C_5Me_4)SiMe_2P(Cy)Ln(CH_2SiMe_3)]_2$[12] (Ln = Y, Lu; Cy = cyclohexyl),[30] which however require careful activation with one equivalent of co-catalyst per dimeric complex. Activation of monomeric complexes $\mathbf{4^{Y}}$ and $\mathbf{4^{Lu}}$ with borate/borane cocatalysts could either produce cationized species devoid of any alkylaluminate moiety or mixed pentadienyl/tetramethylaluminate complexes by abstraction of one pentadienyl ligand (cf., vide supra). Since the generated catalysts are similarly active as the half-sandwich complexes (polymer yields >92%), the 2,4-dimethylpentadienyl ligand (2,4-dmp) is proposed to engage in the polymerization process via a η^5/η^1- coordination switch. The polymers produced by complexes $\mathbf{4^{Ln}}$ display comparatively broad molecular weight distributions M_w/M_n (>1.70) with all three cocatalysts **A**, **B**, and **C** (Table S5). Moreover, relatively high molecular weights ($M_{n,max}$ = 160000) and reduced catalyst efficiencies suggest the formation of a smaller number of active species compared to the half-sandwich precatalysts. The highest *cis* 1,4-selectivities were observed for catalyst system **4**/**C** (max. 89%). In case of precatalyst $\mathbf{4^{Y}}$ the use of double-molar amounts of cocatalyst **A** produced similar polymers as for the equimolar catalyst mixtures.

Conclusions

The formation of rare-earth metal pentadienyl half-sandwich complexes could be achieved via a salt metathesis route and is mainly dependent of the rare-earth metal size and the reaction temperature employed. Rather unexpectedly, the largest rare-earth metal centers selectively formed half-sandwich complexes $[(2,4\text{-dtbp})Ln(AlMe_4)_2]$ (Ln = La, Ce, Pr, Nd), $[(2,4\text{-dipp})La(AlMe_4)_2]$, and $[(2,4\text{-dmp})La(AlMe_4)_2]$, whereas with smaller-sized Ln(III) centers only sandwich complexes $[(2,4\text{-dipp})_2Y(AlMe_4)]$ and $[(2,4\text{-dmp})_2Ln(AlMe_4)]$ (Ln = Y, Lu) could be obtained. Such monomeric half-sandwich complexes feature an η^5-U-shaped coordination of the pentadienyl ligand and distinct tetramethylaluminato coordination in the solid state. Like the cyclopentadienyl-supported half-sandwich complexes, the pentadienyl-supported complexes can be cationized by treatment with perfluorinated borate or borane compounds to form highly active catalyst systems for the homopolymerization of isoprene. Notably the "open" pentadienyl coordination implies in general higher *cis*-1,4-contents than a cyclopentadienyl ancillary environment. Such cationization can be achieved by abstraction of the pentadienyl ligand (with trityl borate $[CPh_3][B(C_6F_5)_4]$) or one methyl group of the $[AlMe_4]$ ligand (with $[PhNMe_2H][B(C_6F_5)_4]$) as evidenced by NMR spectroscopy. Furthermore, a single-component catalyst could be isolated from the equimolar reaction of half-sandwich complex $[(2,4\text{-dtbp})La(AlMe_4)_2]$ with $B(C_6F_5)_3$ via $Me/[C_6F_5]$ exchange. Compared to the C_5Me_5 congener, compound $\{\{(2,4\text{-dtbp})La[(\mu\text{-}Me)_2AlMe(C_6F_5)]\}^+[Me_2Al(C_6F_5)_2]^-\}_2$ features less tightly bonded contact ion pairs which markedly affects the polymerization performance. Overall, the choice of the rare-earth metal and cocatalyst greatly influences the microstructure of the obtained polyisoprenes whereas choice of the pentadienyl ligand seems a less determining factor. Also of note should be that aluminato/gallato exchange of $[(2,4\text{-dtbp})La(AlMe_4)_2]$ with the Lewis acid $GaMe_3$ and Et_2O as a donor led to the corresponding gallate complex $[(2,4\text{-dtbp})La[GaMe_4)_2]$ showing markedly different solid-state features compared to its aluminate precursor.

Experimental Section

General Considerations. All manipulations were performed under rigorous exclusion of air and moisture using standard Schlenk, high-vacuum, and glovebox techniques (MBraun UNIlab^{pro} ECO); <0.5 ppm O_2, <0.5 ppm H_2O, argon atmosphere). The solvents *n*-hexane, toluene, diethyl ether, and tetrahydrofuran (thf) were purified using Grubbs-type columns (MBraun SPS, solvent purification system). C_6D_6 (99.6%, Sigma-Aldrich), and toluene-d_8 (99.6%, Sigma-Aldrich) were dried by letting the solvents stand over Na/K-alloy for at least 24 h and subsequently filtrated. $CDCl_3$ (99.8%, Sigma-Aldrich) was used as received. All solvents were stored inside a glovebox. $Ln(AlMe_4)_3$ (Ln = Y, La, Ce, Pr, Nd, Lu) were synthesized according to literature procedures.[19b,e,31] K(2,4-dmp) was prepared from 2,4-dimethyl-1,3-pentadiene (98%, Sigma-Aldrich) and K/NEt_3 according to a procedure published by Yasuda and co-workers.[2] K(2,4-dtbp) was prepared from 2,4-*tert*-butyl-1,3-pentadiene and Schlosser's base.[3d] Tetramethylsilane was purchased from Sigma-Aldrich, dried over potassium, distilled and stored in a glovebox prior to use. $GaMe_3$ (optoelectronic grade) was purchased from Dockweiler Chemicals and used as received. $[CPh_3][B(C_6F_5)_4]$, $[PhNMe_2H][B(C_6F_5)_4]$, and $B(C_6F_5)_3$ were obtained from Boulder Scientific and used without further purification. NaH, $Ph_3P\text{–}CH_3Br$, *n*-BuLi (2.5 M in *n*-hexane), and DMSO (≥99%) were purchased from Sigma-Aldrich and used as received. 2,5,6-Trimethylhept-4-en-3-one was synthesized according to a literature procedure.[32] NMR spectra of air and moisture sensitive compounds were recorded by using J. Young valve NMR tubes at ambient temperature on either a Bruker AVII+400 (^1H, ^{13}C, ^{19}F) or a Bruker AVII+500 (low temperature spectra). NMR chemical shifts are referenced to internal solvent resonances and reported in parts per million relative to tetramethylsilane (TMS), and CCl_3F. Coupling constants are given in Hertz. Elemental analyses were performed on an Elementar Vario Micro Cube. Size-exclusion

10.1002/chem.201900108

chromatography (SEC) was performed on a Viscotek GPCmax consisting of a GPCmax apparatus and a model TDA 302 triple detector array. Sample solutions (1.0 mg polymer per mL THF) were filtered through a 0.45 μm syringe filter prior to injection. The flow rate was 1 mL/min. d*n*/d*c* and d*A*/d*c* data were determined by means of the integrated OmniSec software. The microstructure of the polyisoprenes was determined on a Bruker AVBII+400 spectrometer in $CDCl_3$ at ambient temperatures. Glass transition temperatures of the polyisoprenes (T_g) were recorded on a Perkin-Elmer DSC 8000, calibrated with cyclohexane and indium standards, and by scanning from –100 °C up to + 100 °C with heating rates of 20 K/min and cooling rates of 60 K/min in N_2 atmosphere.

2,4-Di-*iso*-propyl-1,3-pentadiene. Sodium hydride (2.43 g, 0.10 mol) was placed inside a three-necked flask equipped with a nitrogen inlet and dropping funnel. DMSO (50 mL) was slowly added under vigorous stirring and subsequently heated to 80 °C. After hydrogen evolution had stopped (approx. 0.5 h), the reaction mixture was cooled to ambient temperature and a solution of $Ph_3P–CH_3Br$ (36.1 g, 0.10 mol) in 100 mL of DMSO was added slowly under vigorous stirring. After 10 min 2,5,6-trimethylhept-4-en-3-one (15.4 g, 0.10 mol) was added and the solution heated to 60 °C for 2 h and stirred for another 18 h at ambient temperature. Afterwards, the reaction mixture was poured onto 150 mL of distilled water and extracted 3 times with 50 mL of *n*-hexane. The combined organic phases were washed with water (50 mL), dried over Na_2SO_4 and fractionated under reduced pressure to obtain 2,4-di-*iso*-propyl-1,3-pentadiene as a colorless liquid (9.35 g, 0.06 mol, 61%). B.p. 35 °C (5 mbar); ^1H NMR (400 MHz, $CDCl_3$, 26 °C): δ = 5.65 (d, ^4J(H,H) = 1.18 Hz, 1H; –C*H*=), 4.96 (dd, ^2J(H,H) = 2.27 Hz, ^4J(H,H) = 1.12 Hz, 2H; =C*H*$_{endo}$), 4.67 (dd, ^2J(H,H) = 2.31 Hz, ^4J(H,H) = 1.74 Hz, 2H; =C*H*$_{exo}$), 2.31 (m, 1H; –C*H*(CH_3)$_2$), 2.29 (m, 1H; –C*H*(CH_3)$_2$), 1.70 (s, 3H; –C*H*$_3$), 1.04 (d, ^3J(H,H) = 6.88 Hz, 6H; –CH(C*H*$_3$)$_2$), 1.00 ppm (d, ^3J(H,H) = 6.88 Hz, 6H; –CH(C*H*$_3$)$_2$); $^{13}C\{^1H\}$ NMR (101 MHz, $CDCl_3$, 26 °C): δ = 152.6 (s, 1C; *C*CH(CH_3)$_2$), 144.4 (s, 1C; *C*CH(CH_3)$_2$), 122.6 (s, 1C; –*C*H=), 109.8 (s, 1C; =*C*H_2), 37.4 (s, 1C; C*C*H(CH_3)$_2$), 35.4 (s, 1C; C*C*H(CH_3)$_2$), 21.7 (s, 2C; CCH(*C*H_3)$_2$), 21.6 (s, 2C; CCH(*C*H_3)$_2$), 15.2 ppm (s, 1C; –*C*H_3); elemental analysis calcd (%) for $C_{11}H_{20}$: C 86.76, H 13.24; found: C 84.26, H 12.51. The low carbon and hydrogen values are caused by residual Et_2O.

K(2,4-dipp). KO*t*Bu (6.89 g, 0.06 mol) was suspended in 100 mL of *n*-hexane and the suspension was cooled to –78 °C. To the chilled and stirred suspension, 2,4-di-*iso*-propyl-1,3-pentadiene (9.35 g, 0.06 mol) and subsequently *n*-BuLi (26 mL, 0.07 mol, 2.5 M in *n*-hexane) were added slowly. After complete addition, the reaction mixture was warmed slowly to ambient temperature and stirred for another 18 h. The precipitate was separated off and washed 3 times with 25 mL of *n*-hexane and once with 20 mL of cold THF. After drying in vacuo, K(2,4-dipp) was obtained as an off-white solid (8.20 g, 0.04 mol, 70%). ^1H NMR (400 MHz, [D$_8$]THF, 26 °C): δ = 3.48 (dd, ^4J(H,H) = 2.21 Hz, ^4J(H,H) = 1.84 Hz, 1H; –C*H*=), 3.44 (dd, ^2J(H,H) = 2.50 Hz, ^4J(H,H) = 1.86 Hz, 2H; C*H*$_{exo}$), 3.09 (d, ^2J(H,H) = 1.99 Hz, 2H; C*H*$_{endo}$), 2.13 (m, 2H; –C*H*(CH_3)$_2$), 1.08 ppm (d, ^3J(H,H) = 6.90 Hz, 12H; –CH(C*H*$_3$)$_2$); $^{13}C\{^1H\}$ NMR (101 MHz, [D$_8$]THF, 26 °C): δ = 156.2 (s, 2C; *C*CH(CH_3)$_2$), 79.5 (s, 1C; –*C*H=), 73.3 (s, 2C; =*C*H_2), 40.7 (s, 2C; C*C*H(CH_3)$_2$), 25.0 ppm (s, 2C; CCH(*C*H_3)$_2$); elemental analysis calcd (%) for $C_{11}H_{19}K$: C 69.40, H 10.06; found: C 66.76, H 8.93. Although these results are outside the range viewed as establishing analytical purity, they are provided to illustrate the best values obtained to date.

[2,4-dmp)La(AlMe$_4$)$_2$] (1). To a cooled (–40 °C) and stirred suspension of K(2,4-dmp) (75.5 mg, 0.56 mmol) in 2.5 mL of toluene, an equally cold solution of La(AlMe$_4$)$_3$ (250 mg, 0.63 mmol) in 2.5 mL of toluene was added. The reaction mixture was stirred at –40 °C for 18 h and afterwards the solvent was removed in vacuo. The solid residue was washed 3 times with *n*-hexane (3 mL) and the combined organic phases concentrated to give an orange oil. Th oil was cooled to –40 °C and 0.1 mL of *n*-hexane was added, which led to the formation of a colorless precipitate. The latter was separated via filtration and the process repeated until no more precipitate could be observed. After re-cooling the remaining oil to –40 °C, **1** formed as orange crystals overnight suitable for an X-ray diffraction study. Unfortunately, no crystalline yield can be given due to co-crystallization of unreacted La(AlMe$_4$)$_3$. Yield (determined by ^1H NMR): 74%; ^1H NMR (500 MHz, [D$_8$]toluene, –40 °C): δ = 4.65 (s, 1H; –C*H*=), 3.86 (s, 2H; =C*H*$_{exo}$), 3.37 (s, 2H; =C*H*$_{endo}$), 1.63 (s, 6H; –C*H*$_3$), –0.21 ppm (s, 24H; Al(C*H*$_3$)$_4$); $^{13}C\{^1H\}$ NMR (126 MHz, [D$_8$]toluene, 26 °C): δ = 153.0 (s, 2C; *C*CH$_3$), 95.7 (s, 1C; –*C*H=), 94.2 (s, 2C; =*C*H$_2$), 29.2 (s, 2C; C*C*H$_3$), 1.9 ppm (s, 8C; Al(*C*H$_3$)$_4$). An elemental analysis cannot be provided due to contamination with La(AlMe$_4$)$_3$.

[2,4-dipp)La(AlMe$_4$)$_2$] (2). To a cooled (–40 °C) and stirred suspension of K(2,4-dipp) (85.6 mg, 0.45 mmol) in 2.5 mL of toluene, an equally cold solution of La(AlMe$_4$)$_3$ (200 mg, 0.50 mmol) in 2.5 mL of toluene was added. The reaction mixture was stirred at –40 °C for 18 h and afterwards the solvent was removed in vacuo. The solid residue was washed 3 times with *n*-hexane (3 mL) and the combined organic phases concentrated to yield an orange oil. After addition of tetramethylsilane (0.3 mL), orange crystals of **2** (156 mg, 0.34 mmol, 75%) formed overnight at –40 °C. ^1H NMR (400 MHz, [D$_6$]benzene, 26 °C): δ = 4.71 (t, ^4J(H,H) = 2.20 Hz, 1H; –C*H*=), 4.22 (dd, ^2J(H,H) = 2.62 Hz, ^4J(H,H) = 2.09 Hz, 2H; =C*H*$_{exo}$), 3.62 (d, ^2J(H,H) = 1.92 Hz, 2H; =C*H*$_{endo}$), 2.18 (m, 2H; –C*H*(CH_3)$_2$), 1.02 (d, ^3J(H,H) = 6.87 Hz, 6H; –CH(C*H*$_3$)$_2$), 0.86 (d, ^3J(H,H) = 6.73 Hz, 6H; –CH(C*H*$_3$)$_2$), –0.16 ppm (s, 24H; Al(C*H*$_3$)$_4$); $^{13}C\{^1H\}$ NMR (101 MHz, [D$_6$]benzene, 26 °C): δ = 163.8 (s, 2C; *C*CH(CH_3)$_2$), 94.8 (s, 1C; –*C*H=), 90.8 (s, 2C; =*C*H$_2$), 39.3 (s, 2C; C*C*H(CH_3)$_2$), 25.5 (s, 2C; CCH(*C*H$_3$)$_2$), 20.1 (s, 2C; CCH(*C*H$_3$)$_2$), 1.9 ppm (s, 8C; Al(*C*H$_3$)$_4$); elemental analysis calcd (%) for $C_{19}H_{43}Al_2La$: C 49.14, H 9.33; found: C 48.13, H 8.51. The low carbon and hydrogen values can be explained by residual tetramethylsilane.

[2,4-dtbp)La(AlMe$_4$)$_2$] (3^{La}). To a cooled (–40 °C) and stirred suspension of K(2,4-dtbp) (98.0 mg, 0.45 mmol) in 5 mL of *n*-hexane, an equally cold solution of La(AlMe$_4$)$_3$ (200 mg, 0.50 mmol) in 5 mL of *n*-hexane was added. The reaction mixture was stirred at –40 °C for 2 h and the remaining precipitate was removed via centrifugation and washed 3 times with *n*-hexane (3 mL). The combined organic phases were concentrated to give an orange oil. After addition of tetramethylsilane (0.3 mL), orange crystals of **3^{La}** (172 mg, 0.35 mmol, 78%) formed overnight at –40 °C. ^1H NMR (400 MHz, [D$_6$]benzene, 26 °C): δ = 4.99 (t, ^4J(H,H) = 2.33 Hz, 1H; –C*H*=), 4.33 (dd, ^2J(H,H) = 2.92 Hz, ^4J(H,H) = 2.44 Hz, 2H; =C*H*$_{exo}$), 4.15 (d, ^2J(H,H) = 2.52 Hz, 2H; =C*H*$_{endo}$), 0.95 (s, 18H; –C(C*H*$_3$)$_3$), –0.04 ppm (s, 24H; Al(C*H*$_3$)$_4$); $^{13}C\{^1H\}$ NMR (101 MHz, [D$_6$]benzene, 26 °C): δ = 167.2 (s, 2C; *C*C(CH_3)$_3$), 92.0 (s, 1C; –*C*H=), 90.2 (s, 2C; =*C*H$_2$), 39.4 (s, 2C; C*C*(CH_3)$_3$), 30.4 (s, 6C; CC(*C*H$_3$)$_3$), 4.6 ppm (s, 8C; Al(*C*H$_3$)$_4$); elemental analysis calcd (%) for $C_{21}H_{47}Al_2La$: C 51.22, H 9.62; found: C 51.90, H 9.32.

[2,4-dtbp)Ce(AlMe$_4$)$_2$] (3^{Ce}). To a cooled (–40 °C) and stirred suspension of K(2,4-dtbp) (98.0 mg, 0.45 mmol) in 5 mL of *n*-hexane, an equally cold solution of Ce(AlMe$_4$)$_3$ (200 mg, 0.50 mmol) in 5 mL of *n*-hexane was added. The reaction mixture was stirred at –40 °C for 2 h and the remaining precipitate was removed via centrifugation and washed 3 times with *n*-hexane (3 mL). The combined organic phases were concentrated to give a red oil. After addition of tetramethylsilane (0.3 mL), dark orange crystals of **3^{Ce}** (148 mg, 0.30 mmol, 67%) formed overnight at –40 °C. ^1H NMR (400 MHz, [D$_6$]benzene, 26 °C): δ = 42.26 (s, 1H; –C*H*=), 3.21 (s, 24H; Al(C*H*$_3$)$_4$), 3.03 (s, 18H; –C(C*H*$_3$)$_3$), –16.77 (s, 2H; =C*H*$_2$), –32.85 ppm (s, 2H; =C*H*$_2$); elemental analysis calcd (%) for $C_{21}H_{47}Al_2Ce$: C 51.09, H 9.60; found: C 51.02, H 9.45.

[2,4-dtbp)Pr(AlMe$_4$)$_2$] (3^{Pr}). To a cooled (–40 °C) and stirred suspension of K(2,4-dtbp) (97.7 mg, 0.45 mmol) in 5 mL of *n*-hexane, an equally cold solution of Pr(AlMe$_4$)$_3$ (200 mg, 0.50 mmol) in 5 mL of *n*-hexane was added.

The reaction mixture was stirred at –40 °C for 2 h and the remaining precipitate was removed via centrifugation and washed 3 times with *n*-hexane (3 mL). The combined organic phases were concentrated to give a red oil. After addition of tetramethylsilane (0.3 mL), dark orange crystals of **3**$^{\mathrm{Pr}}$ (108 mg, 0.22 mmol, 45%) formed overnight at –40 °C. ^{1}H NMR (400 MHz, [D$_6$]benzene, 26 °C): δ = 96.48 (s, 1H; –C*H*=), 8.22 (s, 24H; Al(C*H*$_3$)$_4$), 6.29 (s, 18H; –C(C*H*$_3$)$_3$), –48.10 (s, 2H; =C*H*$_2$), –78.99 ppm (s, 2H; =C*H*$_2$); elemental analysis calcd (%) for $\mathrm{C_{21}H_{47}Al_2Pr}$: C 51.01, H 9.58; found: C 50.23, H 9.01.

[2,4-dtbp)Nd(AlMe$_4$)$_2$] (3$^{\mathrm{Nd}}$). To a cooled (–40 °C) and stirred suspension of K(2,4-dtbp) (96.9 mg, 0.44 mmol) in 5 mL of *n*-hexane, an equally cold solution of Nd(AlMe$_4$)$_3$ (200 mg, 0.49 mmol) in 5 mL of *n*-hexane was added. The reaction mixture was stirred at –40 °C for 2 h and the remaining precipitate was removed via centrifugation and washed 3 times with *n*-hexane (3 mL). The combined organic phases were concentrated to give a dark red oil. After addition of tetramethylsilane (0.3 mL), red crystals of **3**$^{\mathrm{Nd}}$ (126 mg, 0.25 mmol, 57%) formed overnight at –40 °C. ^{1}H NMR (400 MHz, [D$_6$]benzene, 26 °C): δ = 44.78 (s, 1H; –C*H*=), 7.99 (s, 24H; Al(C*H*$_3$)$_4$), 3.81 (s, 18H; –C(C*H*$_3$)$_3$), –31.39 (s, 2H; =C*H*$_2$), –45.92 ppm (s, 2H; =C*H*$_2$); elemental analysis calcd (%) for $\mathrm{C_{21}H_{47}Al_2Nd}$: C 50.67, H 9.52; found: C 50.48, H 9.58.

[2,4-dmp)$_2$Y(AlMe$_4$)] (4$^{\mathrm{Y}}$). To a stirred suspension of K(2,4-dmp) (153 mg, 1.14 mmol) in 5 mL of toluene, a solution of Y(AlMe$_4$)$_3$ (200 mg, 0.57 mmol) in 5 mL of toluene was added. The reaction mixture was stirred at ambient temperature for 18 h and afterwards the solvent was removed in vacuo. The solid residue was washed 3 x with *n*-hexane (3 mL) and the combined organic phases concentrated. After standing overnight at –40 °C, yellow crystals of **4**$^{\mathrm{Y}}$ (109 mg, 0.30 mmol, 52%) could be obtained. ^{1}H NMR (400 MHz, [D$_6$]benzene, 26 °C): δ = 4.89 (t, ^{4}*J*(H,H) = 1.98 Hz, 2H; –C*H*=), 3.98 (s, 4H; =C*H*$_{\mathrm{exo}}$), 3.21 (s, 4H; =C*H*$_{\mathrm{endo}}$), 1.69 (s, 12H; –C*H*$_3$), –0.36 ppm (d, ^{2}*J*(H,Y) = 1.78 Hz, 12H; Al(C*H*$_3$)$_4$); ^{13}C{^{1}H} NMR (101 MHz, [D$_6$]benzene, 26 °C): δ = 148.2 (s, 4C; *C*(CH$_3$)), 90.4 (s, 2C; –*C*H=), 86.3 (s, 4C; =*C*H$_2$), 29.2 (s, 4C; C(*C*H$_3$)), 8.8 ppm (s, 4C; Al(*C*H$_3$)$_4$); ^{13}C signals attributable to the [AlMe$_4$] ligand could be resolved with an ^{1}H-^{13}C HSQC NMR experiment; elemental analysis calcd (%) for $\mathrm{C_{18}H_{34}AlY}$: C 59.01, H 9.35; found: C 58.34, H 9.36. The same outcome was observed when the reaction was performed at -40 °C.

[2,4-dmp)$_2$Lu(AlMe$_4$)] (4$^{\mathrm{Lu}}$). To a stirred suspension of K(2,4-dmp) (123 mg, 0.92 mmol) in 5 mL of toluene, a solution of Lu(AlMe$_4$)$_3$ (200 mg, 0.46 mmol) in 5 mL of toluene was added. The reaction mixture was stirred at ambient temperature for 18 h and afterwards the solvent was removed in vacuo. The solid residue was washed 3 times with *n*-hexane (3 mL) and the combined organic phases concentrated. After standing overnight at –40 °C, yellow crystals of **4**$^{\mathrm{Lu}}$ (114 mg, 0.25 mmol, 55%) could be obtained. ^{1}H NMR (400 MHz, [D$_6$]benzene, 26 °C): δ = 4.94 (t, ^{4}*J*(H,H) = 1.95 Hz, 2H; –C*H*=), 3.92 (s, 4H; =C*H*$_{\mathrm{exo}}$), 3.08 (s, 4H; =C*H*$_{\mathrm{endo}}$), 1.76 (s, 12H; –C*H*$_3$), –0.16 ppm (br s, 6H; (μ–*Me*$_2$AlMe$_2$)); –0.34 (br s, 6H; (μ–Me$_2$Al*Me*$_2$)); ^{13}C{^{1}H} NMR (101 MHz, [D$_6$]Benzene, 26 °C): δ = 147.9 (s, 4C; *C*(CH$_3$)), 90.1 (s, 2C; –*C*H=), 84.5 (s, 4C; =*C*H$_2$), 29.2 (s, 4C; C(*C*H$_3$)), 11.6 (s, 2C; (μ–*Me*$_2$AlMe$_2$)); 11.4 ppm (s, 2C; (μ–Me$_2$Al*Me*$_2$)); ^{13}C-signals attributable to the [AlMe$_4$] ligand could be resolved with an ^{1}H-^{13}C HSQC NMR experiment; elemental analysis calcd (%) for $\mathrm{C_{18}H_{34}AlLu}$: C 47.79, H 7.57; found: C 47.31, H 7.05.

[2,4-dipp)$_2$Y(AlMe$_4$)] (5). To a stirred suspension of K(2,4-dipp) (207 mg, 1.08 mmol) in 5 mL of *n*-hexane, a solution of Y(AlMe$_4$)$_3$ (200 mg, 0.57 mmol) in 5 mL of *n*-hexane was added. The reaction mixture was stirred at ambient temperature for 18 h and afterwards the solvent was removed in vacuo. The solid residue was washed 3 times with *n*-hexane (3 mL) and the combined organic phases dried under reduced pressure to obtain **5** as a yellow-green solid (195 mg, 0.41 mmol, 71%). Crystals suitable for X-ray diffraction analysis could be obtained from a concentrated *n*-hexane solution. ^{1}H NMR (400 MHz, [D$_6$]benzene, 26 °C): δ = 4.86 (t, ^{4}*J*(H,H) = 2.00 Hz, 2H; –C*H*=), 4.09 (dd, ^{2}*J*(H,H) = 2.64 Hz, ^{4}*J*(H,H) = 2.05 Hz, 4H; =C*H*$_{\mathrm{exo}}$), 3.38 (d, ^{2}*J*(H,H) = 1.96 Hz, 4H; =C*H*$_{\mathrm{endo}}$), 2.24 (m, 4H; –C*H*(CH$_3$)$_2$), 1.13 (d, ^{2}*J*(H,H) = 6.88 Hz, 12H; –CH(C*H*$_3$)$_2$), 0.97 (d, ^{2}*J*(H,H) = 6.66 Hz, 12H; –CH(C*H*$_3$)$_2$), –0.30 ppm (d, ^{2}*J*(H,Y) = 1.78 Hz, 12H; Al(C*H*$_3$)$_4$); ^{13}C{^{1}H} NMR (101 MHz, [D$_6$]Benzene, 26 °C): δ = 159.5 (s, 4C; *C*CH(CH$_3$)$_2$), 87.4 (s, 2C; –*C*H=), 82.6 (s, 4C; =*C*H$_2$), 38.9 (s, 4C; C*C*H(CH$_3$)$_2$), 25.3 (s, 4C; CCH(*C*H$_3$)$_2$), 20.4 (s, 4C; CCH(*C*H$_3$)$_2$); ^{13}C signals attributable to the [AlMe$_4$] ligand could not be resolved; elemental analysis calcd (%) for $\mathrm{C_{26}H_{50}AlY}$: C 65.25, H 10.53; found: C 65.25, H 10.36.

[2,4-dtbp)$_2$Nd(AlMe$_4$)] (6). To a stirred suspension of K(2,4-dtbp) (100 mg, 0.46 mmol) in 5 mL of *n*-hexane, a solution of Nd(AlMe$_4$)$_3$ (100 mg, 0.57 mmol) in 5 mL of *n*-hexane was added. The reaction mixture was stirred at ambient temperature for 18 h and afterwards the solvent was removed in vacuo. The solid residue was washed 3 times with *n*-hexane (3 mL) and the combined organic phases dried under reduced pressure to obtain **6** as a green solid (123 mg, 0.21 mmol, 85%). Crystals suitable for X-ray diffraction analysis could be obtained from a concentrated *n*-hexane solution. ^{1}H NMR (400 MHz, [D$_6$]benzene, 26 °C): δ = 34.50 (s, 2H; –C*H*=), 4.10 (s, 36H; –C(C*H*$_3$)$_3$), –12.40 (br s, 12H; Al(C*H*$_3$)$_4$), –27.20 (s, 4H; =C*H*$_2$), –34.50 ppm (s, 4H; =C*H*$_2$); elemental analysis calcd (%) for $\mathrm{C_{30}H_{58}AlNd}$: C 61.07, H 9.91; found: C 60.42, H 9.21.

[2,4-dtbp)La(GaMe$_4$)$_2$] (7). To a stirred solution of **3**$^{\mathrm{La}}$ (100 mg, 0.20 mmol) in *n*-hexane (2 mL), GaMe$_3$ (70.0 mg, 0.61 mmol) was added under vigorous stirring at ambient temperature. Subsequently, a solution of GaMe$_3$·Et$_2$O (154 mg; 0.81 mmol) in 1 mL of *n*-hexane was also added and the reaction mixture was stirred for 30 min. at r.t. After concentrating the solution under reduced pressure, cooling to –40 °C, and addition of 0.1 mL of tetramethylsilane, orange crystals of **7** (94.0 mg, 0.16 mmol, 80%) could be obtained. ^{1}H NMR (500 MHz, [D$_6$]benzene, 26 °C): δ = 4.98 (t, ^{4}*J*(H,H) = 2.04 Hz, 1H; –C*H*=), 4.33 (dd, ^{2}*J*(H,H) = 3.15 Hz, ^{4}*J*(H,H) = 2.39 Hz, 2H; =C*H*$_{\mathrm{exo}}$), 4.16 (d, ^{2}*J*(H,H) = 2.34 Hz, 2H; =C*H*$_{\mathrm{endo}}$), 0.97 (s, 18H; –C(C*H*$_3$)$_3$), 0.10 (s, 24H; Ga(C*H*$_3$)$_4$); ^{13}C{^{1}H} NMR (126 MHz, [D$_6$]benzene, 26 °C): δ = 166.3 (s, 2C; *C*C(CH$_3$)$_3$), 90.9 (s, 1C; –*C*H=), 99.3 (s, 2C; =*C*H$_2$), 39.0 (s, 2C; C*C*(CH$_3$)$_3$), 30.2 (s, 6C; CC(*C*H$_3$)$_3$), 6.0 ppm (s, 8C; Ga(*C*H$_3$)$_4$); Elemental analysis cannot be provided due to contamination with an unknown side-product.

{{(2,4-dtbp)La[(μ-Me)$_2$AlMe(C$_6$F$_5$)]}[Me$_2$Al(C$_6$F$_5$)$_2$]}$_2$·(toluene)$_2$ (8). To a stirred solution of **3**$^{\mathrm{La}}$ (50.0 mg, 0.10 mmol) in toluene (1.5 mL), a solution of B(C$_6$F$_5$)$_3$ (52.0 mg, 0.10 mmol) in toluene (1.5 mL) was added. The reaction mixture was stirred for 30 min and then concentrated in vacuo. After cooling to –40 °C, orange crystals of **8** (70 mg, 0.03 mmol, 70%) were obtained. Caution! Owing to the formation of thermal and shock-sensitive [Me$_2$Al(C$_6$F$_5$)$_2$]$^-$, extra care should be taken when handling the dry solid. Crystals have to be dried at normal pressure as drying under reduced pressure causes toluene to be removed from the compound, resulting in unpredictable behavior of the product. ^{1}H NMR (400 MHz, [D$_6$]benzene, 26 °C): δ = 5.08 (s, 2H; –C*H*=), 4.34 (br s, 8H; C*H*$_2$), 0.86 (s, 36H; –C(C*H*$_3$)$_3$), 0.56 (s, 6H; –Al*Me*(C$_6$F$_5$)), 0.19 (s, 24H; –(μ-*Me*)$_2$Al); ^{13}C{^{1}H} NMR (126 MHz, [D$_8$]Toluene, 26 °C): δ = 93.1 (s, 2C; –*C*H=), 91.4 (s, 4C; =*C*H$_2$), 39.3 (s, 4C; C*C*(CH$_3$)$_3$), 29.6 (s, 12C; CC(*C*H$_3$)$_3$), 9.6 (s, 2C; –Al*Me*(C$_6$F$_5$)), 6.4 (s, 8C; –(μ-*Me*)$_2$Al); ^{13}C signals not visible in the ^{13}C{^{1}H} NMR spectrum could be resolved with an ^{1}H-^{13}C HSQC NMR experiment; ^{19}F{^{1}H} NMR (376 MHz, [D$_6$]benzene, 26 °C): δ = –121.8 (br s, 6F; *o*-F), –122.3 (br s, 6F; *o*-F), –153.3 (br s, 3F; *p*-F), –154.0 (br s, 3F; *p*-F), –160.6 (br s, 6F; *m*-F), –161.1 (br s, 6F; *m*-F); elemental analysis calcd (%) for $\mathrm{C_{86}H_{92}F_{30}Al_4La_2}$: C 49.63, H 4.46; found: C 49.77, H 4.16. The discrepancy in toluene content between crystal structure (three molecules of toluene) and elemental analysis (two molecules of toluene) can be attributed to loss of one molecule of toluene upon drying.

Polymerization of Isoprene. A detailed polymerization procedure is described as a typical example. A solution of [CPh$_3$][B(C$_6$F$_5$)$_4$] **(A)** (1 equiv., 18.4 mg, 0.02 mmol) in toluene (3.5 mL) was added to a solution of pre-catalyst $\mathbf{3^{La}}$ (9.98 mg, 0.02 mmol) in toluene (3.5 mL) and the mixture was stirred at ambient temperature for 30 min. After addition of isoprene (2.00 mL, 20 mmol), the polymerization was carried out at ambient temperature for 2 h. The polymerization mixture was quenched in a large quantity (50 mL) of methanol containing 0.1% (w/w) 2,6-di-*tert*-butyl-4-methylphenol as a stabilizer. After washing with methanol, the polymer was dried in vacuo at ambient temperature to constant weight. The monomer conversion was determined gravimetrically. The microstructure of the polymer was examined by ^{1}H and ^{13}C NMR spectroscopy in CDCl$_3$.

X-Ray Crystallography and Crystal Structure Determinations. Crystals of **1**, **2**, $\mathbf{3^{La}}$, $\mathbf{3^{Ce}}$, $\mathbf{3^{Pr}}$, $\mathbf{3^{Nd}}$, $\mathbf{4^{Y}}$, $\mathbf{4^{Lu}}$, **5**, **6**, **7**, **8**, and **Ph$_3$C–(2,4-dtbp)** were grown by standard techniques using saturated solutions of *n*-hexane/TMS (**1**, **2**, $\mathbf{3^{La}}$, $\mathbf{3^{Ce}}$, $\mathbf{3^{Pr}}$, $\mathbf{3^{Nd}}$, **7**), *n*-hexane ($\mathbf{4^{Y}}$, $\mathbf{4^{Lu}}$, **5**, **6**), and toluene (**8, Ph$_3$C–(2,4-dtbp)**). Suitable crystals for X-ray structure analyses were selected in a glovebox and coated with Parabar 10312 (previously known as Paratone N, Hampton Research) and fixed on a nylon/loop glass fiber. X-ray data for compounds **1** to **8** were collected on a Bruker APEX III DUO instrument equipped with an IµS microfocus sealed tube and QUAZAR optics for MoKα (λ = 0.71073 Å) and CuKα (λ = 1.54184 Å) radiation. The data collection strategy was determined using COSMO[33] employing ω-scans. Raw data were processed using APEX[34] and SAINT[35], corrections for absorption effects were applied using SADABS[36]. The structures were solved by direct methods and refined against all data by full-matrix least-squares methods on F^2 using SHELXTL[37] and SHELXLE[38]. All graphics were produced employing CCDC Mercury 3.10.1[39]. Further details regarding the refinement and crystallographic data are listed in Tables S1-S3 and in the CIF files. CCDC depositions 1886707-1886718 contain all the supplementary crystallographic data for this paper. These data can be obtained free of charge from The Cambridge Crystallographic Data Centre via www.ccdc.cam.ac.uk/data_request/cif.

Acknowledgements

We are grateful to the German Science Foundation (An 238/14-2) and Bridgestone Japan for generous support.

Keywords: lanthanides • pentadienyl ligand • isoprene polymerization • half-sandwich complex •

[1] J. E. Mahler, R. Pettit, *J. Am. Chem. Soc.* **1962**, *84*, 1511-1512.

[2] Y. Hajime, O. Yasuo, Y. Michihide, T. Hisaya, N. Akira, *Bull. Chem. Soc. Jpn.* **1979**, *52*, 2036-2045.

[3] a) Y. Hajime, O. Yasuo, N. Akira, K. Yasushi, Y. Noritake, K. Nobutami, *Bull. Chem. Soc. Jpn* **1980**, *53*, 1101-1111; b) Y. Hajime, Y. Michihide, N. Akira, S. Tsuyoshi, K. Yasushi, Y. Noritake, K. Nobutami, *Bull. Chem. Soc. Jpn.* **1980**, *53*,1089-1100; c) J. S. Overby, T. P. Hanusa, *Angew. Chem. Int. Ed. Engl.* **1994**, *33*, 2191-2193; d) M. Reiners, A. C. Fecker, M. Freytag, P. G. Jones, M. D. Walter, *Dalton Trans.* **2014**, *43*, 6614-6617.

[4] a) R. D. Ernst, *Acc. Chem. Res.* **1985**, *18*, 56-62; b) R. D. Ernst, *Chem. Rev.* **1988**, *88*, 1255-1291; c) R. D. Ernst, *Comments Inorganic Chem.* **1999**, *21*, 285-325; d) L. Stahl, R. D. Ernst, *Adv. Organometal. Chem., Vol. 55* (Eds.: R. West, A. F. Hill, M. J. Fink), Academic Press, **2007**, pp. 137-199.

[5] M. Reiners, D. Baabe, P. Schweyen, M. Freytag, P. G. Jones, M. D. Walter, *Inorg. Chim. Acta* **2014**, *422*, 167-180.

[6] a) P. Powell, *J. Chem. Res., Synopses* **1978**; b) P. Powell, *J. Organomet. Chem.* **1981**, *206*, 239-255; c) P. Powell, *J. Organomet. Chem.* **1983**, *244*, 393-399; d) A. Ceccon, A. Gambaro, A. Venzo, *J. Chem. Soc., Chem. Commun.* **1985**, 540-542; e) P. Powell, M. Stephens, A. Muller, M. G. B. Drew, *J. Organomet. Chem.* **1986**, *310*, 255-268; f) W. A. Donaldson, M. Ramaswamy, *Tetrahedron Letters* **1989**, *30*, 1339-1342; g) R. A. Fischer, W. A. Herrmann, *J. Organomet. Chem.* **1989**, *377*, 275-279; h) V. Kulsomphob, G. C. Turpin, K.-C. Lam, C. Youngkin, W. Trakarnpruk, P. Carroll, A. L. Rheingold, R. D. Ernst, *J. Chem. Soc., Dalton Trans.* **2000**, 3086-3093.

[7] W. Trakarnpruk, A. M. Arif, R. D. Ernst, *Organometallics* **1992**, *11*, 1686-1692.

[8] a) W. A. Donaldson, P. T. Bell, M.-J. Jin, *J. Organomet. Chem.* **1992**, *441*, 449-456; b) R. W. Gedridge, A. M. Arif, R. D. Ernst, *J. Organomet. Chem.* **1995**, *501*, 95-100.

[9] a) W. Trakarnpruk, A. L. Rheingold, B. S. Haggerty, R. D. Ernst, *Organometallics* **1994**, *13*, 3914-3920; b) V. Kulsomphob, K. A. Ernst, K.-C. Lam, A. L. Rheingold, R. D. Ernst, *Inorg. Chim. Acta* **1999**, *296*, 170-175.

[10] a) E. A. Benham, P. D. Smith, E. T. Hsieh, M. P. McDaniel, *J. Macromol. Sci. A.* **1988**, *25*, 259-283; b) P. D. Smith, M. P. McDaniel, *J. Polym. Sci. A.* **1989**, *27*, 2695-2710.

[11] a) R. D. Ernst, T. H. Cymbaluk, *Organometallics* **1982**, *1*, 708-713; b) N. Hu, L. Gong, Z. Jin, W. Chen, *Wuji Huaxue Xuebao* **1989**, *5*, 107-111; c) Q. Xin, L. Ju-Zheng, *Chin. J. Chem.* **1991**, *9*, 10-19; d) D. Baudry, F. Nief, L. Ricard, *J. Organomet. Chem.* **1994**, *482*, 125-130; e) M. B. Zielinski, D. K. Drummond, P. S. Iyer, J. T. Leman, W. J. Evans, *Organometallics* **1995**, *14*, 3724-3731; f) S. Zhang, D. Cui, J. Cheng, J. Jin, N. Hu, W. Chen, J. Liu, *Yingyong Huaxue* **2001**, *18*, 330-335; g) M. R. Kunze, D. Steinborn, K. Merzweiler, C. Wagner, J. Sieler, R. Taube, *Z. Anorg. Allg. Chem.* **2007**, *633*, 1451-1463.

[12] R. H. Chen, P. Wang, Q. Liu, Y. H. Dong, Y. Y. Li, *Chinese J. Inorg. Chem.* **2015**, *31*, 1239-1244.

[13] K. Kunze, A. M. Arif, R. D. Ernst, *Bull. Soc. Chim. Fr.* **1993**, *130*, 708-711.

[14] a) J. Jin, S. Jin, Z. Jin, W. Chen, *J. Chem. Soc., Chem. Commun.* **1991**, 1328-1329; b) S. Zhang, J. Jin, G. Wei, W. Chen, J. Liu, *J. Organomet. Chem.* **1994**, *483*, 57-60.

[15] J. Sieler, A. Simon, K. Peters, R. Taube, M. Geitner, *J. Organomet. Chem.* **1989**, *362*, 297-303.

[16] M. R. Kunze, R. Taube, *Z. Anorg. Allg. Chem.* **2010**, *636*, 2454-2461.

[17] a) F. Bonnet, M. Visseaux, A. Pereira, D. Barbier-Baudry, *Macromolecules* **2005**, *38*, 3162-3169; b) D. Robert, T. P. Spaniol, J. Okuda, *Eur. J. Inorg. Chem.* **2008**, *2008*, 2801-2809; c) M. Zimmermann, K. W. Törnroos, R. Anwander, *Angew. Chem., Int. Ed.* **2008**, *47*, 775-778; d) M. Zimmermann, K. W. Törnroos, H. Sitzmann, R. Anwander, *Chem. – Eur. J.* **2008**, *14*, 7266-7277; e) M. Zimmermann, J. Volbeda, K. W. Törnroos, R. Anwander, *Comptes Rendus Chimie* **2010**, *13*, 651-660. f) D. Li, S. Li, D. Cui, X. Zhang, *Organometallics* **2010**, *9*, 2186-2193. g) L. Li, C. Wu, D. Liu, S. Li, D. Cui, *Organometallics* **2013**, *11*, 3203-3209. h) L. Guo, X. Zhu, G. Zhang, Y. Wei, L. Ning, S. Zhou, Z. Feng, S. Wang, X. Mu, J. Chen, Y. Jiang, *Inorg. Chem.* **2015**, *54*, 5725-5731. i) G. Zhang, S. Wang, S. Zhou, Y. Wei, L. Guo, X. Zhu, L. Zhang, X. Gu, X. Mu, *Organometallics* **2015**, *17*, 4251-4261. j) G. Zhang, Y. Wei, L. Guo, X. Zhu, S. Wang, S. Zhuo, X. Mu, *Chem. – Eur. J.* **2015**, *21*, 2519-2526. k) G. Zhang, B. Deng, S. Wang, Y. Wei, S. Zhou, X. Zhu, Z. Huang, X. Mu, *Dalton Trans.* **2016**, *45*, 15445-15456. l) C. Yu, D. Zhou, X. Yan, F. Gao, L. Zhang, S. Zhang, X. Li, *Polymers* **2017**, *9*, 531/1-531/11.

[18] a) S. Zhiquan, J. Ouyang, in *Handbook on the Physics and Chemistry of Rare Earths, Vol. 9*, Elsevier, **1987**, pp. 395-428; b) L. Porri, G. Ricci, A. Giarrusso, N. Shubin, Z. Lu, in *Olefin Polymerization, Vol. 749*, American Chemical Society, **1999**, pp. 15-30; c) R. Taube, G. Sylvester, in *Applied Homogeneous Catalysis with Organometallic Compounds* (Eds.: B. Cornils, W. A. Herrmann), **2002**; d) K. Osakada, D. Takeuchi, in *Polymer Synthesis*, Springer Berlin Heidelberg, **2004**, pp. 137-194; e) A. Fischbach, R. Anwander, *Adv. Polym. Sci.* **2006**, 155-281; f) L. Friebe, O. Nuyken, W. Obrecht, in *Adv. Polym. Sci.* (Ed.: O. Nuyken), Springer Berlin Heidelberg, **2006**, pp. 1-154; g) M. Nishiura, Z. Hou, *Nat. Chem.* **2010**, *2*, 257; h) Z. Zhang, D. Cui, B. Wang, B. Liu, Y. Yang, in *Molecular Catalysis of Rare-Earth Elements* (Ed.: P. W. Roesky), Springer Berlin Heidelberg, **2010**, pp. 49-108; i) M. Zimmermann, R. Anwander, *Chem. Rev.* **2010**, *110*, 6194-6259; j) M. Nishiura, F. Guo, Z. Hou, *Acc. Chem. Res.* **2015**, *48*, 2209-2220; k) F. Yang, X. Li, *J. Polym. Sci. A.* **2017**, *55*, 2271-2280; l) J. Jothieswaran, S. Fadlallah, F. Bonnet, M. Visseaux, *Catalysts* **2017**, *7*, 378/1-378/14. m) J. Huang, Z. Liu, D. Cui, X. Liu, *ChemCatChem* **2018**, *10*, 42-61.

[19] a) A. Fischbach, G. Klimpel Michael, M. Widenmeyer, E. Herdtweck, W. Scherer, R. Anwander, *Angew. Chem., Int. Ed.* **2004**, *43*, 2234-2239; b) M. Zimmermann, N. Å. Frøystein, A. Fischbach, P. Sirsch, H. M. Dietrich, K. W. Törnroos, E. Herdtweck, R. Anwander, *Chem. – Eur. J.* **2007**, *13*, 8784-8800; c) L. Zhang, T. Suzuki, Y. Luo, M. Nishiura, Z. Hou, *Angew. Chem., Int. Ed.* **2007**, *46*, 1909-1913; d) W. Gao, D. Cui, *J. Am. Chem. Soc.* **2008**, *130*, 4984-4991; e) C. Hollfelder, L. Jende, D. Diether, T. Zelger, R. Stauder, C. Maichle-Mössmer, R. Anwander, *Catalysts* **2018**, *8*, 61.

[20] a) R. Litlabo, H. S. Lee, M. Niemeyer, K. W. Tornroos, R. Anwander, *Dalton Trans.* **2010**, *39*, 6815-6825; b) L. N. Jende, C. Maichle-Mössmer, R. Anwander, *Chem. – Eur. J.* **2013**, *19*, 16321-16333; c) N. Dettenrieder, C. O. Hollfelder, L. N. Jende, C. Maichle-Mössmer, R. Anwander,

Organometallics **2014**, *33*, 1528-1531; d) L. N. Jende, C. O. Hollfelder, C. Maichle-Mössmer, R. Anwander, *Organometallics* **2015**, *34*, 32-41; e) D. Diether, K. Tyulyunov, C. Maichle-Mössmer, R. Anwander, *Organometallics* **2017**, *36*, 4649-4659.

[21] H. M. Dietrich, C. Zapilko, E. Herdtweck, R. Anwander, *Organometallics* **2005**, *24*, 5767-5771.

[22] E. Le Roux, F. Nief, F. Jaroschik, K. W. Tornroos, R. Anwander, *Dalton Trans.* **2007**, 4866-4870.

[23]a) J. Raeder, M. Reiners, R. Baumgarten, K. Münster, D. Baabe, M. Freytag, P. G. Jones, M. D. Walter, *Dalton Trans.* **2018**; b) D. Barisic, D. Schneider, C. Maichle-Mössmer, R. Anwander, *Angew. Chem., Int. Ed.* **2018**.

[24] J. Wang, Y. Mu, Z. Shi, S. Zhang, S. Feng, *Gaodeng Xuexiao Huaxue Xuebao* **2000**, *21*, 829-831.

[25] H. M. Dietrich, K. W. Törnroos, E. Herdtweck, R. Anwander, *Organometallics* **2009**, *28*, 6739-6749.

[26] H. M. Dietrich, C. Maichle-Mossmer, R. Anwander, *Dalton Trans.* **2010**, *39*, 5783-5785.

[27]a) O. Tardif, S. Kaita, *Dalton Trans.* **2008**, 2531-2533; b) X. Xin, C. Yaofeng, S. Jie, *Chem. – Eur. J.* **2009**, *15*, 846-850.

[28] M. Terrier, M. Visseaux, T. Chenal, A. Mortreux, *J. Polym. Sci. A.* **2007**, *45*, 2400-2409.

[29] a) S. Kaita, Z. Hou, Y. Wakatsuki, *Macromolecules* **1999**, *32*, 9078-9079; b) S. Kaita, Z. Hou, M. Nishiura, Y. Doi, J. Kurazumi, A. C. Horiuchi, Y. Wakatsuki, *Macromol. Rapid Commun.* **2003**, *24*, 179-184; c) S. Kaita, Y. Doi, K. Kaneko, A. C. Horiuchi, Y. Wakatsuki, *Macromolecules* **2004**, *37*, 5860-5862; d) S. Kaita, M. Yamanaka, A. C. Horiuchi, Y. Wakatsuki, *Macromolecules* **2006**, *39*, 1359-1363.

[30] L. Zhang, Y. Luo, Z. Hou, *J. Am. Chem. Soc.* **2005**, *127*, 14562-14563.

[31] G. Occhipinti, C. Meermann, H. M. Dietrich, R. Litlabø, F. Auras, K. W. Törnroos, C. Maichle-Mössmer, V. R. Jensen, R. Anwander, *J. Am. Chem. Soc.* **2011**, *133*, 6323-6337.

[32] M. B. Santelli, Marcel, *Bull. Soc. Chim. Fr.* **1973**, *7-8*, 2326-2330.

[33] COSMO, v. 1.61; BRUKER AXS Inc., Madison, WI, 2012.

[34] APEX 3, v. 2016.5-0; BRUKER AXS Inc., Madison, WI, 2012.

[35] SAINT, v. 8.34A; BRUKER AXS Inc., Madison, WI, 2010.

[36] L. Krause, R. Herbst-Irmer, G. M. Sheldrick, D. Stalke, *J. Appl. Crystallogr.* **2015**, *48*, 3-10.

[37] G. Sheldrick, *Acta Cryst., Sect. A* **2015**, *71*, 3-8.

[38] C. B. Hubschle, G. M. Sheldrick, B. Dittrich, *J. Appl. Crystallogr.* **2011**, *44*, 1281-1284.

[39] C. F. Macrae, I. J. Bruno, J. A. Chisholm, P. R. Edgington, P. McCabe, E. Pidcock, L. Rodriguez-Monge, R. Taylor, J. van de Streek, P. A. Wood *J. Appl. Cryst.* **2008**, *41*, 466-470.

Entry for the Table of Contents

FULL PAPER

Equimolar treatment of open half-sandwich complex [(2,4-dtbp)Ln(AlMe$_4$)$_2$] with B(C$_6$F$_5$)$_3$ gives isolable compound {{(2,4-dtbp)La[(μ-Me)$_2$AlMe(C$_6$F$_5$)]}[Me$_2$Al(C$_6$F$_5$)$_2$]}$_2$ with less tightly bonded contact ion pairs compared to the C$_5$Me$_5$ congener, which markedly affects the polymerization performance.

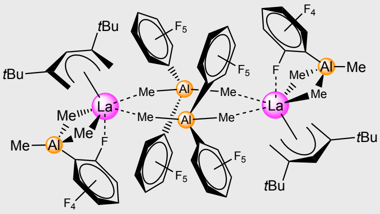

single-component catalyst

*Damir Barisic, Dennis A. Buschmann, David Schneider, Cäcilia Maichle-Mössmer, and Reiner Anwander**

Page No. – Page No.

Rare-Earth-Metal Pentadienyl Half-Sandwich and Sandwich Tetramethylaluminates – Synthesis, Structure, Reactivity, and Performance in Isoprene Polymerization